Particle trajectories: equations of motion, canonical and non-canonical formulation

Xavier Garbet

▶ **To cite this version:**

Xavier Garbet. Particle trajectories: equations of motion, canonical and non-canonical formulation. Doctoral. France. 2023. hal-03974974

HAL Id: hal-03974974
https://hal.science/hal-03974974v1

Submitted on 6 Feb 2023

HAL is a multi-disciplinary open access archive for the deposit and dissemination of scientific research documents, whether they are published or not. The documents may come from teaching and research institutions in France or abroad, or from public or private research centers.

L'archive ouverte pluridisciplinaire **HAL**, est destinée au dépôt et à la diffusion de documents scientifiques de niveau recherche, publiés ou non, émanant des établissements d'enseignement et de recherche français ou étrangers, des laboratoires publics ou privés.

Distributed under a Creative Commons Attribution - NonCommercial - NoDerivatives 4.0 International License

Particle trajectories: equations of motion, canonical and non-canonical formulation

X. Garbet[1,2]

[1]CEA, IRFM, Saint-Paul-lez-Durance, F-13108, France

[2]School of Physical and Mathematical Sciences, Nanyang Technological University, 637371 Singapore

February 6, 2023

Abstract

This note presents different descriptions of the equations of motion of a charged particle subject to an electromagnetic field. Variational principles are given in their Lagrangian and Hamiltonian forms. A non-canonical form is determined in the special case of a strong magnetic guide-field. Conditions for integrability and existence of angle/action variables are derived and discussed. This methodology is applied to the tokamak magnetic configuration. Trajectories are explicitly calculated in the limit of small orbit width. Corresponding angle/action variables are constructed.

1 Trajectories of charged particles in a electromagnetic field

Computing particle trajectories in a inhomogeneous electromagnetic magnetic field is mandatory since this issue is at the heart of magnetic confinement. This problem is a difficult one, and not often solvable analytically. The objective is to compute the motion of a particle in the phase space given by its position $\mathbf{x}(t)$ and velocity $\mathbf{v}(t) = \dot{\mathbf{x}}(t)$ (the dot indicates a time derivative) for a set of initial conditions $(\mathbf{x}_0, \mathbf{v}_0)$. Fortunately, in most practical problems, this question can be recast in a tractable way thanks to powerful theorems of Lagrangian and Hamiltonian mechanics.

1.1 Newtonian, Lagrangian and Hamiltonian descriptions

Several ways exists to write the trajectory equations of a charged particle in an electromagnetic field. If relativistic effects are discarded, the Newtonian formulation is the obvious starting point

$$\begin{aligned} \frac{d\mathbf{x}}{dt} &= \mathbf{v} \\ m_a \frac{d\mathbf{v}}{dt} &= e_a \left[\mathbf{E}\left(\mathbf{x},t\right) + \mathbf{v} \times \mathbf{B}\left(\mathbf{x},t\right)\right] \end{aligned}$$

where m_a and e_a are the particle mass and algebraic charge, $\mathbf{E}(\mathbf{x},t)$ the electric field, and $\mathbf{B}(\mathbf{x},t)$ the magnetic field. An equivalent formulation relies on a principle of least action

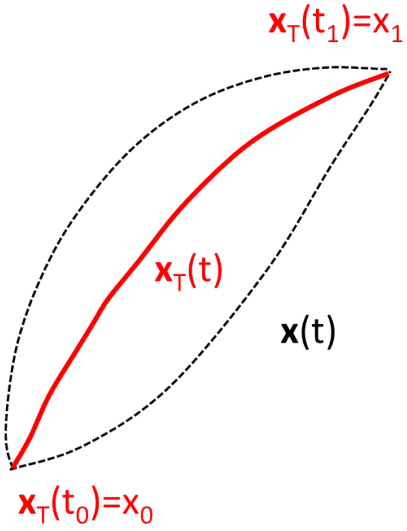

Figure 1: Possible paths (dashed black) that connect the positions x_0 at $t = t_0$ and x_1 at $t = t_1$ in the vicinity of the actual trajectory $x_T(t)$ (solid red).

[1, 2], where the action is defined as

$$\mathcal{A} = \int_{t_0}^{t_1} dt L\left(\mathbf{x}(t), \dot{\mathbf{x}}(t), t\right)$$

with $L(\mathbf{x}, \dot{\mathbf{x}}, t)$ the Lagrangian. A path is a trajectory $\mathbf{x}(t)$ such that $\mathbf{x}(t_0) = \mathbf{x}_0$ and $\mathbf{x}(t_1) = \mathbf{x}_1$, where $\mathbf{x}_0$ and $\mathbf{x}_1$ are given. The principle of least action states that $\delta\mathcal{A} = 0$ for paths $\mathbf{x}(t)$ in the neighbourhood of the actual trajectory $\mathbf{x}_T(t)$, i.e. at first order in any displacement $\delta\mathbf{x}(t) = \mathbf{x}(t) - \mathbf{x}_T(t)$, with $\delta\mathbf{x}(t_0) = \delta\mathbf{x}(t_1) = 0$ (see Fig.1) . Each vector $\mathbf{x}$ is labelled by 3 coordinates x^i (contravariant components). The action variation reads

$$\begin{aligned}\delta\mathcal{A} &= \int_{t_0}^{t_1} dt \left[\frac{\partial L}{\partial x^i}\delta x^i + \frac{\partial L}{\partial v^i}\frac{d\delta x^i}{dt}\right] \\ &= \int_{t_0}^{t_1} dt \delta x^i \left[\frac{\partial L}{\partial x^i} - \frac{d}{dt}\left(\frac{\partial L}{\partial v^i}\right)\right]\end{aligned}$$

where an integration by part has been performed in time, combined with the boundary conditions $\delta\mathbf{x}(t_0) = \delta\mathbf{x}(t_1) = 0$. The principle of least action provides the Euler-Lagrange equations of motion

$$\frac{d}{dt}\left(\frac{\partial L}{\partial \dot{x}^i}\right) = \frac{\partial L}{\partial x^i}$$

where $p_i = \frac{\partial L}{\partial \dot{x}^i}$ is the canonical momentum. The particle Lagrangian for a charged particle subject to an electromagnetic field reads

$$L\left(\mathbf{x}, \mathbf{v}, t\right) = \frac{1}{2} m_a v^2 - e_a \left[\phi\left(\mathbf{x}, t\right) - \mathbf{v} \cdot \mathbf{A}\left(\mathbf{x}, t\right)\right]$$

with $\mathbf{v} = \dot{\mathbf{x}}$, ϕ the electric potential and $\mathbf{A}$ the vector potential. Beyond its elegance, the Lagrangian formulation immediately proves that if the Lagrangian L does not depend on some coordinate x^k, then the corresponding momentum $p_k = \frac{\partial L}{\partial v^k}$ is an invariant of motion, a consequence of the first Noether theorem (see [3] for a derivation of the Noether theorem in the framework of Hamiltonian dynamics). The canonical momentum in presence of an electromagnetic field is $\mathbf{p} = m_a\mathbf{v} + e_a\mathbf{A}\left(\mathbf{x}, t\right)$, hence not as simple as $\mathbf{p} = m_a\mathbf{v}$ that would apply for a force free motion - this is particularly important in fusion devices where the electromagnetic part is much larger than the velocity part i.e. $|e_a| A \gg m_a v$. It is

sometimes preferable to use the canonical momentum $\mathbf{p}$ instead of the velocity $\mathbf{v}$. The variable $\mathbf{p}$ is said conjugate to $\mathbf{x}$. This is done by building a particle Hamiltonian $H(\mathbf{x},\mathbf{p},t)$ from its Lagrangian counterpart L via a Legendre transform $H(\mathbf{x},\mathbf{p},t) = \mathbf{p}\cdot\mathbf{v} - L(\mathbf{x},\mathbf{v},t)$. The Hamilton equations of motion are

$$\begin{aligned} \frac{dx^i}{dt} &= \frac{\partial H}{\partial p_i} \\ \frac{dp_i}{dt} &= -\frac{\partial H}{\partial x^i} \end{aligned} \tag{1}$$

One useful additional evolution equation is $\frac{dH}{dt} = -\frac{\partial L}{\partial t}$. The Hamiltonian is $H(\mathbf{x},\mathbf{p},t) = \frac{1}{2m_a}\left[\mathbf{p} - e_a\mathbf{A}(\mathbf{x},t)\right]^2 + e_a\phi(\mathbf{x},t)$ for a charged particle moving in an electromagnetic field. The antisymmetry of Eq.(1) is characteristics of Hamiltonian dynamical systems, and more generally of the underlying symplectic geometry. A number of results are available (see overviews [2, 3]), which we will be used without derivation.

One important part of Hamiltonian mechanics deals with canonical transforms, i.e. changes of variables that respect the structure Eq.(1). Let us call $(\bar{\mathbf{x}},\bar{\mathbf{p}})$ a new set of canonical variables. The canonical coordinates $(\bar{\mathbf{x}},\bar{\mathbf{p}})$ are functions of $(\mathbf{x},\mathbf{p})$ that verify the following properties[1]

$$\left\{\bar{x}^i,\bar{x}^j\right\} = 0 \quad ; \quad \{\bar{p}_i,\bar{p}_j\} = 0 \quad ; \quad \left\{\bar{x}^i,\bar{p}_j\right\} = \delta_i^j$$

and

$$\oint_{\mathcal{C}} \mathbf{p}\cdot d\mathbf{x} = \oint_{\mathcal{C}} \bar{\mathbf{p}}\cdot d\bar{\mathbf{x}}$$

where $\mathcal{C}$ is a closed contour in the phase space[2]. Next question is then to build a set of canonical conjugate coordinates $(\bar{\mathbf{x}},\bar{\mathbf{p}})$ when a set $(\mathbf{x},\mathbf{p})$ is known. One way is to use the Hamilton principle of least action. The new Lagrangian reads $\bar{L} = \bar{\mathbf{p}}\cdot\dot{\bar{\mathbf{x}}} - \bar{H}(\bar{\mathbf{x}},\bar{\mathbf{p}},t)$, where $\bar{H}$ is the new Hamiltonian. Moreover the action $\bar{\mathcal{A}} = \int_{t_0}^{t_1} dt\bar{L}$ must satisfy $\delta\bar{\mathcal{A}} = 0$. One sufficient condition to enforce this condition is to relate the two Lagrangians via the relation $L = \bar{L} + d\mathcal{S}$, where the generating function $\mathcal{S}$ is differentiable, so that the two actions differ by a constant. The generating function $\mathcal{S}$ depends on variables from the first set $(\mathbf{x},\mathbf{p})$, and other variables from the second set $(\bar{\mathbf{x}},\bar{\mathbf{p}})$. Let us consider for instance the combination $\mathcal{S} = S(\mathbf{x},\bar{\mathbf{p}},t) - \bar{\mathbf{x}}\cdot\bar{\mathbf{p}}$, another example of Legendre transform. It then appears that

$$\begin{aligned} \bar{x}^i &= \frac{\partial S}{\partial \bar{p}_i} \\ p_i &= \frac{\partial S}{\partial x^i} \\ \bar{H} &= H + \frac{\partial S}{\partial t} \end{aligned}$$

Four formulations are possible, which correspond to various possible Legendre transformations. This provides a convenient way of building a new set of conjugate variables from a known one.

1.2 Integrability and angle-action variables

In spite of their elegance, Hamiltonian or Lagrangian formulations still require solving a set of 6 ordinary differential equations - a formidable task. Fortunately simplifications

[1] This property means in practice that a Poisson bracket expressed in the variables $(\bar{\mathbf{x}},\bar{\mathbf{p}})$ has the same expression as in $(\mathbf{x},\mathbf{p})$.

[2] More generally Poincaré integrals $\int..\int\int_S \sum dx^i dp_i ... dx^j dp_j dx^k dp_k$, where S is a $2n$ surface in the phase space, can be shown to be invariant through a change of canonical coordinates.

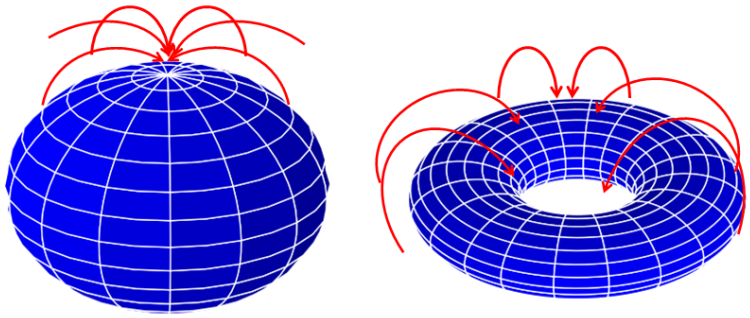

Figure 2: Hairy ball theorem. Red lines represents oriented hairs - a sphere cannot be combed without forming singularities (here at the poles) whereas a torus can.

occur in some specific cases, of relevance for fusion plasmas. A well known theorem in dynamical systems states that a motion is integrable if there exists 3 invariants of motion [3]. "Integrable" means that the trajectory equations can be formally written with "simple" mathematical tools such a integrals, square roots, etc... If the trajectories are bounded, then the invariant manifold is compact. Another theorem then states that under reasonable conditions (e.g. flow smoothness on the invariant manifold, no singularity), a compact manifold in a 6D phase space has to be a 3-dimensional torus, i.e. the generalization of a doughnut in a 6 dimensional space (this is known as the "hairy ball" or "hedgehog" theorem - see Fig.2) . These are called invariant tori. On top of it, it can be shown that it is possible to construct a set action/angle variables, i.e. to replace the set of canonically conjugate variables $(\mathbf{x}, \mathbf{p})$ by a new set $(\boldsymbol{\alpha}, \mathbf{J})$ such that

$$\begin{aligned} \frac{d\alpha^i}{dt} &= \frac{\partial H}{\partial J_i} = \Omega^i \\ \frac{dJ_i}{dt} &= -\frac{\partial H}{\partial \alpha^i} = 0 \end{aligned}$$

where the Hamiltonian H depends on the 3 actions J_i only. The 3 pulsations Ω^i are called angular pulsations. In this very special case, trajectories take a pleasant form $\alpha^i = \Omega^i t + \alpha^i_0$, and $J_i = J_{i0}$, where the 6 numbers $\left(\alpha^i_0, J_{i0}\right)$ are set by the initial conditions. This apparent simplicity should not hide the real difficulty, namely the explicit calculation of angle/action variables as function of the initial set of variables $(\mathbf{x}, \mathbf{p})$ (or $(\mathbf{x}, \mathbf{v})$).

1.3 Non canonical coordinates

The Lagrange/Hamilton formulation of the equations of motion may appear as quite restrictive regarding the choice of the variables $(\mathbf{x}, \mathbf{v})$ or $(\mathbf{x}, \mathbf{p})$. Ideally one would like to use an arbitrary set of 6 coordinates z^i. This appears to be crucial when solving numerically the equations of motion. Fortunately the principle of least action offers a

powerful way to find the equations of motion [4]. The particle Lagrangian is of the form[3]

$$L(\mathbf{z}, \dot{\mathbf{z}}, t) = \gamma_i(\mathbf{z}, t)\dot{z}^i - h(\mathbf{z}, t)$$

where

$$\gamma_i(\mathbf{z}, t) = \mathbf{p} \cdot \frac{\partial \mathbf{x}}{\partial z^i}$$

and

$$h(\mathbf{z}, t) = H(\mathbf{x}, \mathbf{p}, t) - \mathbf{p} \cdot \frac{\partial \mathbf{x}}{\partial t}$$

The initial conjugate variables $(\mathbf{x}, \mathbf{p})$ are now functions of $(\mathbf{z}, t)$. The principle of least action leads to the equations

$$\omega_{ij}\frac{dz^j}{dt} = \frac{\partial h}{\partial z^i} + \frac{\partial \gamma_i}{\partial t}$$

where $\omega_{ij} = \frac{\partial \gamma_j}{\partial z^i} - \frac{\partial \gamma_i}{\partial z^j}$ are the Lagrange brackets of the coordinates z^i

$$\omega_{ij} = [z_i, z_j] = \frac{\partial \mathbf{p}}{\partial z^i} \cdot \frac{\partial \mathbf{x}}{\partial z^j} - \frac{\partial \mathbf{p}}{\partial z^j} \cdot \frac{\partial \mathbf{x}}{\partial z^i}$$

Defining J^{ij} as the inverse matrix of ω_{ij}, each element J^{ij} is a Poisson bracket

$$\mathrm{J}^{ij} = \left\{z^i, z^j\right\} = \frac{\partial z^i}{\partial \mathbf{x}} \cdot \frac{\partial z^j}{\partial \mathbf{p}} - \frac{\partial z^j}{\partial \mathbf{p}} \cdot \frac{\partial z^i}{\partial \mathbf{x}}$$

The Poisson bracket of two functions $f(\mathbf{z}, t)$ and $g(\mathbf{z}, t)$ is defined as $\{f, g\} = \frac{\partial f}{\partial z^i} J^{ij} \frac{\partial f}{\partial z^j}$, or equivalently the conventional form

$$\{f, g\} = \frac{\partial f}{\partial \mathbf{x}} \cdot \frac{\partial g}{\partial \mathbf{p}} - \frac{\partial f}{\partial \mathbf{p}} \cdot \frac{\partial g}{\partial \mathbf{x}}$$

The equations of motion can then be written as

$$\frac{dz^i}{dt} = \left\{z^i, h\right\} + \left\{z^i, z^j\right\}\frac{\partial \gamma_j}{\partial t}$$

Of course these relations apply in the special case where the z^i are a set of conjugate variables $(\bar{\mathbf{x}}, \bar{\mathbf{p}})$. The Liouville theorem states that the Jacobian $\sqrt{g} = [det(\omega_{ij})]^{1/2}$ is conserved by the flow, i.e.

$$\frac{\partial \sqrt{g}}{\partial t} + \frac{\partial}{\partial z^i}\left(\sqrt{g}\dot{z}^i\right) = 0$$

2 Guiding-centre description

2.1 Guiding-centre Lagrangian

Solving the equations of motion is usually quite challenging. Fortunately, magnetised plasmas are characterized by a strong magnetic guide field, that is chosen slowly evolving in time (and so is the unperturbed electric field). "Strong" means here that the local particle gyroradius[4] $\rho_c = \frac{m_a v_\perp}{e_a B(\mathbf{x})}$ ($v_\perp$ is the perpendicular velocity) is small enough compared with a field gradient length L_B (typically $L_B = |\nabla \ln B(\mathbf{x}, t)|^{-1}$), i.e. $\epsilon_B = \frac{\rho_c}{L_B} \ll 1$ [5].

[3] Doubled indices are summed.

[4] The reader is supposed here to be accustomed with the cyclotron motion of a charged particle in a uniform magnetic field.

[5] This is a rather loose definition of a strong guide-field. There exists counter-examples where $\epsilon_B \ll 1$, ans still the guiding-centre does not apply. Traditionally the normalised gyroradius to the plasma size a is noted ρ_*, i.e. $\rho_* = \frac{\rho_c}{a}$. If the field spatial variation scales as the plasma size, then $\epsilon_B \sim \rho_*$.

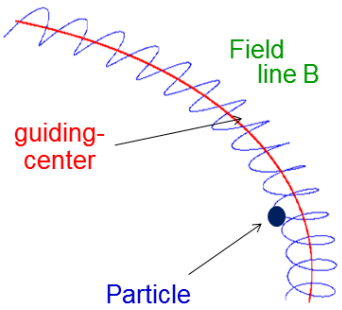

Figure 3: Decomposition of a particle trajectory as a combination of guiding-centre and cyclotron motions.

The ordering is such that the magnitude of the guide-field is $\frac{1}{\epsilon_B}$, and its time variation is $o(\epsilon_B)$[6]. The trajectory can then be written as the sum of a guiding centre motion $\mathbf{X}$ and a cyclotron motion $\mathbf{x}(t) = \mathbf{X}(t) + \epsilon_B \boldsymbol{\rho}(t)$, where $\boldsymbol{\rho}(t)$ is a periodic function of a cyclotron angle (as shown on Fig.3)

$$\varsigma = \frac{1}{\epsilon_B} \int^t dt' \Omega_c \left[\mathbf{X}(t'), \epsilon_B t'\right] + \varsigma_0$$

Here $\Omega_c = e_a B\left(\mathbf{X}, \epsilon_B t\right)/m_a$ is the local cyclotron pulsation ("local" in the sense that it is calculated at the position of the guiding-centre), and ς_0 the initial cyclotron phase. A major result is that an "adiabatic invariant" $\mu\left(\mathbf{x}, \mathbf{p}\right)$ can be built at "all orders" in ϵ_B [5, 6], in the form of an asymptotic development in ϵ_B [7]. At order one in the small parameter ϵ_B, the cyclotron motion reads

$$\boldsymbol{\rho}_0(t) = \rho_c \left(\cos\varsigma\, \mathbf{e}_1 - \sin\varsigma\, \mathbf{e}_2\right) \quad (2)$$

$$\dot{\boldsymbol{\rho}}_0(t) = v_\perp \left(-\sin\varsigma\, \mathbf{e}_1 - \cos\varsigma\, \mathbf{e}_2\right) \quad (3)$$

where $\mathbf{e}_1\left(\mathbf{X}\right), \mathbf{e}_2\left(\mathbf{X}\right)$ are two unit vectors locally orthogonal to the magnetic field $\mathbf{B}\left(\mathbf{X}, \epsilon_B t\right)$. The adiabatic invariant appears to be the particle magnetic moment[8]

$$\mu\left(\mathbf{x}, \mathbf{v}\right) = \frac{m_a v_\perp^2}{2B\left(\mathbf{X}\right)}$$

[6]The parameter ϵ_B is from now on a dumb variable used to identify the order of the various terms and perform the expansion in a rigorous way. It is set to 1 at the end of the calculation to get the equations of motion.

[7]An asymptotic series is by no mean similar to a conventional Taylor development. In a Taylor development, the largest the number of terms the better the accuracy for small arguments. In contrast an asymptotic development is characterized by a optimum number of terms depending on the argument. Hence there is no need to push the development too far if the argument is not small enough. Also two different functions may be represented by the same asymptotic series.

[8]The cyclotron motion of a charged particle can be seen as a current that generates a dipolar magnetic field, as would do a magnet with a magnetic dipole moment $\mu = \frac{1}{2}\rho_c^2 e_a \Omega_c$, aligned with the local magnetic field.

It is worth spending a while on the conventions and signs adopted here, in particular in Eqs.(3). The cyclotron angle ς is *anti-trigonometric*, while $d\varsigma/dt = \epsilon_B^{-1}\Omega_c$, with $\Omega_c(\mathbf{X}) = eB(\mathbf{X})/m$. This just reflects that ions rotate in the anti-trigonometric direction with respect to the magnetic field $\mathbf{B}$, while electrons rotate in the counter-trigonometric direction (see Fig.4). The perpendicular velocity $v_\perp$ is a norm and is always positive, it reads $v_\perp = \sqrt{2\mu B/m_a}$. On the other hand, the gyroradius $\rho_c = \frac{m_a v_\perp}{e_a B}$ and cyclotron angular frequency $\Omega_c = \frac{e_a B}{m_a}$ changes sign with the particle charge. Writing $\boldsymbol{\rho}_0 = \rho_c \mathbf{e}_\rho$ and $\dot{\boldsymbol{\rho}}_0 = v_\perp \mathbf{e}_v$, the basis $(\mathbf{e}_\rho, \mathbf{e}_\parallel, \mathbf{e}_v)$ is orthogonal and direct.

The guiding-centre coordinates that characterize the motion of a charged particle are $z^i = \left(\mathbf{X}, u_\parallel, \mu, \varsigma\right)$, $u_\parallel$ is the parallel velocity of the guiding centre[9]. Starting from the $6D$ Lagrangian $L\left(\mathbf{x}, \mathbf{p}, t\right) = \mathbf{p}\cdot\dot{\mathbf{x}} - H$, it was shown by Littlejohn [7] that the Lagrangian for the set of variables z^i is[10]

$$L\left(\mathbf{z}, t\right) = \frac{1}{\epsilon_B} e_a \mathbf{A}^* \cdot \dot{\mathbf{X}} + \epsilon_B \frac{m_a}{e_a} \mu\dot{\varsigma} - H \tag{4}$$

where ϵ_B is kept here to visualize the ordering, but should be set to 1 once all calculations are done[11]. The Hamiltonian is

$$H = \frac{1}{2} m_a u_\parallel^2 + \mu B\left(\mathbf{X}, \epsilon_B t\right) + e_a \phi\left(\mathbf{X}, \epsilon_B t\right)$$

where ϕ is the equilibrium electric potential. The modified vector potential is

$$\mathbf{A}^*\left(\mathbf{X}, \epsilon_B t\right) = \mathbf{A}\left(\mathbf{X}, \epsilon_B t\right) + \frac{m_a u_\parallel}{e_a} \mathbf{e}_\parallel\left(\mathbf{X}, \epsilon_B t\right)$$

where $\mathbf{e}_\parallel$ is the local unit vector along the field line $\mathbf{e}_\parallel\left(\mathbf{x}, \epsilon_B t\right) = \frac{\mathbf{B}(\mathbf{x}, \epsilon_B t)}{B(\mathbf{x}, \epsilon_B t)}$.

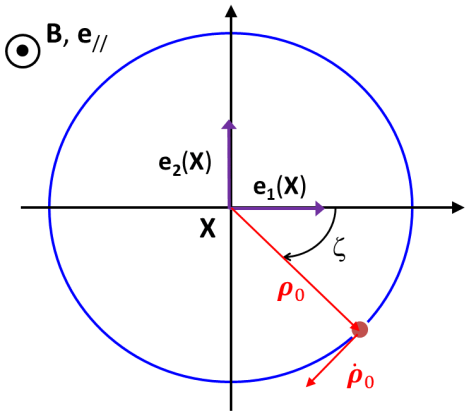

Figure 4: Geometric conventions for a cyclotron trajectory.

[9]The velocity $u_\parallel$ may differ from the particle velocity $v_\parallel$, hence a different notation. However at order 1 in ϵ_B both coincides.

[10]A rigorous demonstration can be found in the paper by Littlejohn. A taste of it can be found by using a dynamical argument $\mathbf{A}(\mathbf{x}) = \mathbf{A}(\mathbf{x}_G) + \epsilon_B(\boldsymbol{\rho}_0 \cdot \nabla)\mathbf{A}(\mathbf{x}_G)$, $\dot{\mathbf{x}} = \dot{\mathbf{X}} + \epsilon_B \dot{\boldsymbol{\rho}}_0$, $\mathbf{v} = u_\parallel \mathbf{e}_\parallel + \mathbf{v}_c$. Assuming the cyclotron motion is given by Eq.(3), then $\dot{\boldsymbol{\rho}}_0 = -\dot{\varsigma}\mathbf{e}_\parallel \times \boldsymbol{\rho}_0$. An average over the fast cyclotron motion yields $\langle (m_a \mathbf{v}_c + e_a(\boldsymbol{\rho}_0 \cdot \nabla)\mathbf{A}(\mathbf{x}_G)) \cdot \dot{\boldsymbol{\rho}}_0 \rangle_c = \frac{m_a}{e_a}\mu\dot{\varsigma}$ and the Lagrangian Eq.(4). This is not a rigorous demonstration since it *precludes* the form of the fast cyclotron motion. Littlejohn's demonstration is geometrical and does not rely on dynamical averages. Consequently adiabatic invariance is demonstrated in a rigorous way.

[11]Second order in ϵ_B is given in [7, 8], but not reproduced here

2.2 Equations of motion in the guiding-centre description

The equations of motions are obtained with the Euler-Lagrangian equation computed with the Lagrangian Eq.(4)

$$\frac{d}{dt}\left(\frac{\partial L}{\partial \dot{z}^i}\right) = \frac{\partial L}{\partial z^i}$$

The cyclotron motion is associated with the variables (μ, ς). The corresponding equations of motion are obtained for $z^i = \mu$ and $z^i = \varsigma$, namely

$$\begin{aligned} \frac{d\varsigma}{dt} &= \frac{1}{\epsilon_B}\frac{e_a B(\mathbf{X})}{m_a} = \frac{1}{\epsilon_B}\Omega_c(\mathbf{X}) \\ \frac{d\mu}{dt} &= 0 \end{aligned}$$

The choice $z^i = u_\parallel$ provides the constraint $u_\parallel = \mathbf{e}_\parallel \cdot \mathbf{X}$, consistently with the interpretation of $u_\parallel$ as the parallel velocity of the guiding-centre. The equations of motion of the guiding centre are (after setting $\epsilon_B = 1$)[12]

$$\begin{aligned} B^*_\parallel \frac{d\mathbf{X}}{dt} &= u_\parallel \mathbf{B}^* + \frac{\mathbf{B}}{e_a B} \times (\mu \nabla B - e_a \mathbf{E}^*) \\ B^*_\parallel m_a \frac{du_\parallel}{dt} &= -\mathbf{B}^* \cdot (\mu \nabla B - e_a \mathbf{E}^*) \end{aligned}$$

where

$$\mathbf{B}^* = \nabla \times \mathbf{A}^* = \mathbf{B} + \frac{m_a u_\parallel}{e_a} \nabla \times \mathbf{e}_\parallel$$

and

$$B^*_\parallel = \mathbf{e}_\parallel \cdot \mathbf{B}^* = B + \frac{m_a u_\parallel}{e_a} \mathbf{e}_\parallel \cdot \nabla \times \mathbf{e}_\parallel$$

are the modified magnetic field and its projection along the parallel direction. The modified electric field is

$$\mathbf{E}^* = -\frac{\partial \mathbf{A}^*}{\partial t} - \nabla \phi$$

The Poisson brackets reads[13]

$$\left\{\varsigma, \tfrac{m_a}{e_a}\mu\right\} = 1 \quad ; \quad \left\{X^i, X^j\right\} = -\tfrac{\epsilon^{ijk}}{e_a B}\tfrac{B_k}{B^*_\parallel} \quad ; \quad \left\{\mathbf{X}, m_a u_\parallel\right\} = \tfrac{\mathbf{B}^*}{B^*_\parallel}$$

where ϵ^{ijk} is the Levi-Civita tensor. These relations provide the general expression of the Poisson bracket of two functions expressed in the set of guiding-center variables

$$\begin{aligned} \{f, g\} &= \frac{e_a}{m_a}\left(\frac{\partial f}{\partial \varsigma}\frac{\partial g}{\partial \mu} - \frac{\partial f}{\partial \mu}\frac{\partial g}{\partial \varsigma}\right) \\ &\quad + \frac{1}{m_a}\frac{\mathbf{B}^*}{B^*_\parallel} \cdot \left(\frac{\partial f}{\partial \mathbf{X}}\frac{\partial g}{\partial u_\parallel} - \frac{\partial f}{\partial u_\parallel}\frac{\partial g}{\partial \mathbf{X}}\right) \\ &\quad - \frac{\mathbf{e}_\parallel}{e_a B^*_\parallel} \cdot \left(\frac{\partial f}{\partial \mathbf{X}} \times \frac{\partial g}{\partial \mathbf{X}}\right) \end{aligned}$$

The equations of motion are given by $\frac{dz^i}{dt} = -\left\{H, z^i\right\}$. The Jacobian of the guiding centre system of coordinates is $B^*_\parallel$.

[12] This calculation is most easily done by noting that $\nabla(\mathbf{v} \cdot \mathbf{A}) = \mathbf{v} \times \mathbf{B} + (\mathbf{v} \cdot \nabla)\mathbf{A}$ for any field $\mathbf{v}$ that does not depends on $\mathbf{x}$, and $\mathbf{B} = \nabla \times \mathbf{A}$. The resulting equation is $m_a \dot{u}_\parallel \mathbf{e}_\parallel = e_a \mathbf{E}^* + \epsilon_B^{-1} e_a \dot{\mathbf{X}} \times \mathbf{B} - \mu \nabla B$. The equations of motion are obtained after a projection on $\mathbf{B}^*$ and a cross-product with $\mathbf{e}_\parallel$.

[13] This can be done by comparing the equations of motions with the brackets $-\left\{H, z^i\right\}$, or by building the matrix of Lagrange brackets ω_{ij} and inverting it to find the Poisson brackets J^{ij}.

The special static case presents also some interest, at least in fusion devices where the magnetic field is in quasi-steady state during part of the discharge

$$\begin{aligned} B^*_{||}\frac{d\mathbf{X}}{dt} &= u_{||}\mathbf{B}^* + \frac{1}{e_a}\mathbf{e}_{||}\times\nabla\left(\mu B + e_a\phi\right) \\ B^*_{||}m_a\frac{du_{||}}{dt} &= -\mathbf{B}^*\cdot\nabla\left(\mu B + e_a\phi\right) \end{aligned}$$

2.3 Connection with classical expressions of guiding-centre drift velocities and forces

The guiding-centre velocity $\frac{d\mathbf{X}}{dt}$ can be recast in the form[14]

$$\dot{\mathbf{X}} = u_{||}\mathbf{e}_{||} + \mathbf{v}_D + \mathbf{v}_E$$

where

$$\mathbf{v}_D = \frac{1}{e_a B^*_{||}}\frac{\mathbf{B}}{B}\times\left(m_a u^2_{||}\boldsymbol{\kappa} + \mu\nabla B\right)$$

is the magnetic drift velocity and

$$\mathbf{v}_E = \frac{1}{B^*_{||}}\frac{\mathbf{E}\times\mathbf{B}}{B}$$

the $E\times B$ drift velocity. The magnetic and $E\times B$ drift velocities coincide with classical expressions when $B^*_{||} = B$. Since the difference between the two is of order ϵ_B, this may appear as an acceptable approximation. However it should be remembered that $B^*_{||}$ is the Jacobian of the guiding-centre transform. Hence this approximation would break the constraint of volume conservation - not a consequence to treat lightly. The reader is sent to classical textbooks regarding the physical interpretation of drift velocities [9, 10]. In most magnetic configurations where the toroidal field is dominant, the curvature is directed towards the vertical axis, and the magnetic drift is nearly vertical (see Fig.5).
The equation of motion of the parallel velocity is also of some interest. If one restricts the analysis to the lowest order in ϵ_B, i.e. $\mathbf{B}^* = \mathbf{B}$, $B^*_{||} = B$, then the parallel force balance equation reads

$$m_a\frac{du_{||}}{dt} = -\mathbf{e}_{||}\cdot\nabla\left(\mu B + e_a\phi\right)$$

This expression is commonly encountered in the literature. While the parallel electric force $-e_a\mathbf{e}_{||}\cdot\nabla\phi$ is expected, the first part $-\mu\mathbf{e}_{||}\cdot\nabla B$ may be more surprising. It can be understood by noting that a gyrating charged particle in a strong magnetic field acts as a small magnet with a magnetization μ. The force $-\mu\nabla B$ is the one expected for a magnet plunged in a inhomogeneous magnetic field. This force can accelerate or slow down a charged particle depending on the sign of the field amplitude gradient. If the magnetic field exhibits a minimum, a particle can be trapped near the potential well μB. This force can therefore be used to confine particles. Magnetic bottles are a well known example of this principle. The force $-\mu\nabla B$ is sometimes called "mirror force".

[14] This is most easily verified by using the identity $\nabla\times\mathbf{e}_{||} = \left(\mathbf{e}_{||}\cdot\nabla\times\mathbf{e}_{||}\right)\mathbf{e}_{||} + \mathbf{e}_{||}\times\boldsymbol{\kappa}$, where $\boldsymbol{\kappa} = \left(\mathbf{e}_{||}\cdot\nabla\right)\mathbf{e}_{||}$ is the field line curvature. This leads to the convenient expression $\mathbf{B}^*/B^*_{||} = \mathbf{e}_{||} + \left(m_a u_{||}/e_a B^*_{||}\right)\mathbf{e}_{||}\times\boldsymbol{\kappa}$. The modified electric field can also be written as $\mathbf{E}^* = \mathbf{E} - m_a u_{||}/e_a\partial_t\mathbf{e}_{||}$ - the last term can be neglected for a quasi-steady magnetic field.

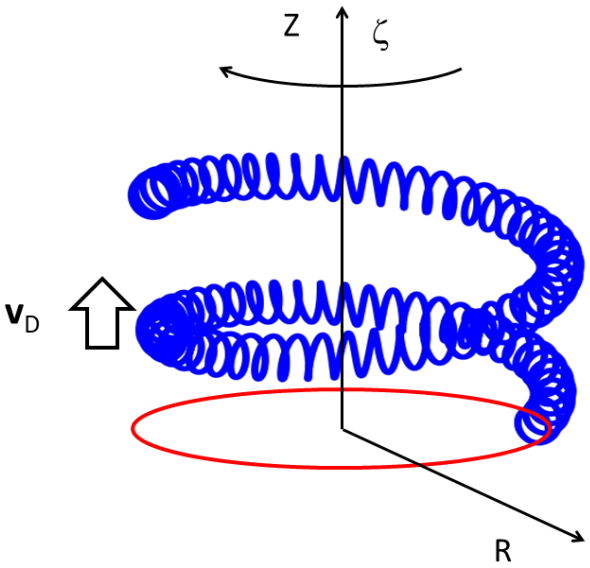

Figure 5: Decomposition of a particle trajectory as the sum of a guiding-centre and cyclotron motion.

3 Application to confining magnetic configurations

3.1 Hamiltonian guiding centre equations*

The structure of the guiding-centre equations of motion show that the variables (ς, μ) form a couple of conjugate variables since $\{\varsigma, m_a\mu/e_a\} = 1$ and the Poisson brackets with all guiding-centre coordinates are null. Hence the equations of motions of the guiding-centre coordinates $(\mathbf{X}, u_\parallel)$ can be treated separately. It is attractive to build a set of canonical conjugate variables, to replace the set $(\mathbf{X}, u_\parallel)$. The Hamiltonian structure of the equations allows using well established results in Hamiltonian mechanics, in particular the condition for transition to chaos (KAM theorem) [6]. It appears this is possible in a magnetic configuration that possesses magnetic surfaces. The guiding-centre part of the Lagrangian Eq.(4) (i.e. removing the cyclotron angle) reads

$$L\left(\mathbf{Z}, t\right) = \left(e_a\mathbf{A} + \frac{m_a u_\parallel}{B}\mathbf{B}\right) \cdot \dot{\mathbf{X}} - H \tag{5}$$

This Lagrangian requires the covariant coordinates of the vector potential and the magnetic field. The covariant coordinates A_i of the vector potential are easily obtained from its expression when using straight field lines coordinates (θ, ζ)

$$\mathbf{A} = \chi(\psi)\nabla\theta - \psi\nabla\zeta \tag{6}$$

The corresponding magnetic field is

$$\mathbf{B} = \nabla\chi(\psi) \times \nabla\theta + \nabla\zeta \times \nabla\psi \tag{7}$$

Eq.(7) provides the contravariant coordinates of the field. A covariant expression would rather be of the form

$$\mathbf{B} = B_\psi\nabla\psi + B_\theta\nabla\theta + B_\zeta\nabla\zeta$$

A convenient way to derive the covariant components field is to use a set of Boozer coordinates (ψ, θ, ζ), which preserves the structure of the magnetic field $\mathbf{B} = \nabla\left(\zeta - q(\psi)\theta\right) \times \nabla\psi$

and is such that $B_\theta = G(\psi)$ and $B_\zeta = I(\psi)$, while B_ψ remains a function of ψ and θ. This change of coordinates brings a convenient form of the Lagrangian[15]

$$L(\mathbf{Z}, t) = m_a u_\parallel \frac{B_\psi}{B}\dot{\psi} + P_\theta \dot{\theta} + P_\zeta \dot{\zeta} - H$$

where

$$P_\theta = e_a \chi + m_a u_\parallel \frac{G}{B}$$

and

$$P_\zeta = -e_a \psi + m_a u_\parallel \frac{I}{B}$$

where $\mathbf{Z} = (\psi, \theta, \zeta)$ are coordinates of the guiding-centre [16]. Obviously the structure is not fully canonical because of the term $\dot{\psi}$. Several recipes have been proposed to circumvent this difficulty, most relying on a change of field coordinates. We adopt here the transform proposed in [11], which consists in modifying the toroidal angle in the following manner

$$\zeta = \bar{\zeta} + \tilde{\zeta}(\psi, \theta)$$

where the function $\tilde{\zeta}$ is chosen such that[17]

$$\frac{\partial \tilde{\zeta}}{\partial \psi} = -\frac{B_\psi(\psi, \theta)}{I(\psi)}$$

The Lagrangian becomes

$$L(\mathbf{Z}, t) = \frac{dS}{dt} + \bar{P}_\theta \dot{\theta} + P_\zeta \dot{\bar{\zeta}} - H \tag{8}$$

where the function S, similar to a generating function, is given by

$$S(\psi, \theta) = -e_a \int^\psi d\psi' \psi' \frac{\partial \tilde{\zeta}}{\partial \psi}$$

and the new action $\bar{P}_\theta$ is

$$\begin{aligned} \bar{P}_\theta &= e_a \chi(\psi) + e_a \int^\psi d\psi' \frac{\partial \tilde{\zeta}}{\partial \theta}(\psi', \theta) \\ &\quad + m_a u_\parallel \left[G(\psi) - I(\psi) \frac{\partial \tilde{\zeta}}{\partial \theta}(\psi, \theta) \right] \end{aligned}$$

The function S can be incorporated in the Lagrangian L since it is transparent when seeking the extremum of the action. Removing the overlines to simplify the notations ($\bar{P}_\theta \to P_\theta$, $\bar{\zeta} \to \zeta$), the new Lagrangian becomes

$$L = P_\theta \dot{\theta} + P_\zeta \dot{\zeta} - H$$

which has the requested structure. In particular the equations of motion are quite handy

$$\begin{array}{ccc} \frac{d\theta}{dt} = \frac{\partial H}{\partial P_\theta} & ; & \frac{dP_\theta}{dt} = -\frac{\partial H}{\partial \theta} \\ \frac{d\zeta}{dt} = \frac{\partial H}{\partial P_\zeta} & ; & \frac{dP_\zeta}{dt} = -\frac{\partial H}{\partial \zeta} \end{array}$$

[15] The parallel velocity $u_\parallel$ is sometimes replaced by the variable $\rho_\parallel = \frac{m_a u_\parallel}{e_a B}$ - a gyroradius built with a parallel velocity. This allows more compact notations.

[16] Strictly speaking, other notations should be chosen for the guiding-centre coordinates since (ψ, θ, ζ) designate in principle the particle coordinates. However there is no ambiguity since the guiding-centre transform has already been done at this point.

[17] The function $\tilde{\zeta}$ plays a similar role as $\widehat{\zeta}$ in the system of angle/action variables. It describes the non uniform precession drift of particles. This effect is usually considered as feeble, so that ζ and $\bar{\zeta}$ are often set equal.

However this approach has limitations too. Indeed the Hamiltonian is usually not known as function of $(\theta, P_\theta, \zeta, P_\zeta)$. This difficulty is overcome by solving first the guiding-centre equations of motion in the variables $z^i = (\psi, \theta, \zeta, v_\parallel)$, and then computing the time variations of (P_θ, P_ζ) from their expressions versus the z^is. The advantage of this choice of coordinates is to better visualise the breakdown of dynamical invariants when perturbations are added. The rationale of this approach is summarized on Fig.6

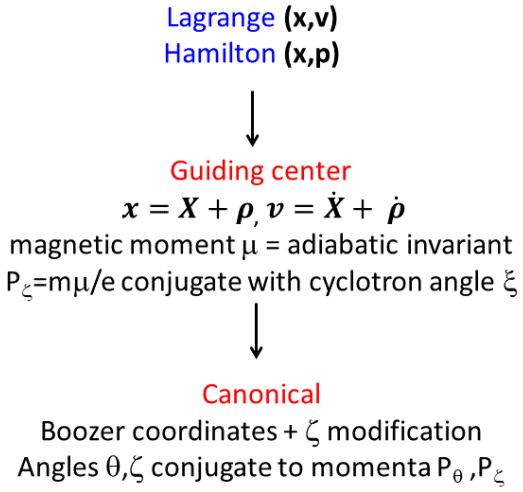

Figure 6: Rationale to build a set of canonically conjugate variables in a confining configuration.

3.2 Symmetry and integrability

Solving guiding-centre equations of motions, in their Hamiltonian form of not, remains a hard task as it requires solving a 4D set of ordinary differential equations parametrized by the magnetic moment. Fortunately other considerations help, at least in the case where the electromagnetic field is static. In this case the particle energy $H_{eq} = \frac{1}{2} m_a u_\parallel^2 + \mu B(\mathbf{X}) + e_a \phi(\mathbf{X})$ is an invariant of motion. Moreover, if the considered system is invariant under some symmetry transform, the first Noether theorem states that a third invariant exist, on top of the particle magnetic moment μ and energy H_{eq}. This is the case in axisymmetric configurations like a tokamak for instance, where the equilibrium magnetic and electric fields do not depend on the toroidal angle φ, i.e. the configuration is left invariant by a rotation around the vertical axis of the torus. In this case, the canonical toroidal momentum $P_\varphi = e_a A_\varphi(\mathbf{X}) + m_a I u_\parallel / B$, where $A_\varphi(\mathbf{X})$ is the toroidal covariant component of the vector potential. In practice this means that particles move on manifolds in the 6 D phase space $(\mathbf{x}, \mathbf{p})$ labelled by $H_{eq}(\mathbf{x}, \mathbf{p}), \mu(\mathbf{x}, \mathbf{p}), P_\varphi(\mathbf{x}, \mathbf{p}) = \mathbf{cte}$, where **cte** is a set of 3 constants specified by the initial conditions. This is an essential step, as now the problem is reduced to a 3D motion on this manifold, that we call invariant manifold. As mentioned before, a powerful theorem by Arnold proves that this motion is integrable. Moreover, it appears that the second piece $m_a \dot{X}_\varphi$ in P_φ is smaller than the first bit $e_a A_\varphi$ by a factor $\epsilon = \rho_*$. The surfaces $A_\varphi = cte$ are bounded in a tokamak (magnetic surfaces), implying that guiding centre trajectories must be bounded. No singularities are expected and the flow is smooth. This means that the invariant manifold is compact. A second theorem [3] (see also the introduction by [12]) then states this compact manifold has to be 3 D torus, i.e. the generalization of a doughnut in a 6 dimensional space. It is thus

known in advance that a set of angle/action variables can be built. This is an essential result, that is detailed now for tokamaks (or any other axisymmetric configuration)[18].

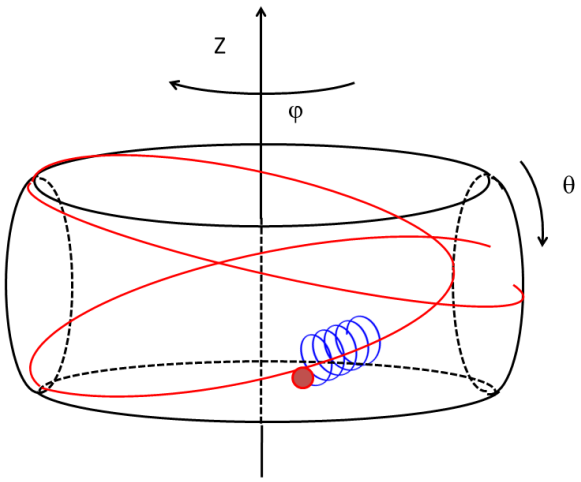

Figure 7: Schematic trajectory of a charged particle in a tokamak.

3.3 Trajectory of a charged particle in a tokamak

3.3.1 Trapped and passing particles

The analysis is restricted to the limit of thin orbit width (which corresponds to $\rho_* \ll 1$). The calculation is then run order per order in ρ_*:

- the cyclotron motion, with a typical pulsation $\Omega_c = \frac{e_a B}{m}$.
- the motion of the guiding-centre along a field line, ignoring the magnetic drift. The typical pulsation is a transit frequency $\frac{u_\parallel}{R}$.
- the effect of the magnetic drift, with a typical frequency $\frac{v_D}{R}$.

Particles are categorised as "passing" or "trapped" depending whether the parallel velocity goes down to zero due to the mirror force. A null point in parallel velocity corresponds to a particle guiding-centre that stops, then moves backward along the field line. In an up-down symmetric equilibrium, the existence of a bounce poloidal angle $\theta = \theta_b$ implies that $\theta = -\theta_b$ is also a bounce point. Hence the corresponding particle moves back and forth between between the poloidal angles $\pm\theta_b$. This is why it is called "trapped". Particles that are not trapped, i.e. move forward or backward, are dubbed "passing". This behaviour is better understood by looking at the energy

$$E = \frac{1}{2} m_a u_\parallel^2 + \mu B(\psi, \theta) + e_a \phi(\psi) \tag{9}$$

and the canonical toroidal momentum

$$P_\varphi = -e_a \psi + \frac{m_a}{B(\psi, \theta)} I(\psi) u_\parallel \tag{10}$$

[18]The situation is less simple for stellarators. If the Hamiltonian exhibits some symmetry, as would be the case for a quasi-symmetric stellarator, the system is still integrable, and a set of angle/action variables can be built. At the least, angles/actions can be built for some classes of particles like mirror trapped particles.

where $I(\psi) = R^2(\mathbf{B}\cdot\nabla\varphi)$. The second piece of the canonical toroidal momentum Eq.(10) is ρ_* smaller than the first part $-e_a\psi$. This means that at first sight the particle guiding-centre stays close to a reference magnetic surface $-P_\varphi/e_a$, labelled ψ_*. In practice this is equivalent to ignore the magnetic drift. The energy Eq.(9) must then be calculated at $\psi = \psi_*$. Moreover, the equation of motion of the guiding-centre poloidal angle is

$$\frac{d\theta}{dt} = u_\parallel \frac{\mathbf{B}\cdot\nabla\theta}{B}$$

where the magnetic drift has been discarded, and the r.h.s. is calculated at $\psi = \psi_*$. Hence the energy Eq.(9) depends on $\left(\mu, \psi_*, \frac{d\theta}{dt}, \theta\right)$. It describes an autonomous motion in θ. The magnetic field on the reference magnetic surface ψ_* spans an interval $[B_{min}, B_{max}]$. If $E - e_a\phi(\psi_*) > \mu B_{max}$, there is no poloidal position such that $u_\parallel = 0$, hence the particle is passing. If $\mu B_{min} < E - e_a\phi(\psi_*) < \mu B_{max}$, then there exists bounce points $\pm\theta_b$ such that $u_\parallel = 0$. Hence the particle is trapped. The effective potential μB acts as a magnetic well, as illustrated in Fig.8. Since the guiding-centre follows a field line, the toroidal angle is just $\varphi = q(\psi_*)\theta + \varphi_0$, where φ_0 is an initial condition. In both cases, passing or trapped, the motion along the field line is periodic and can be characterised by an angle and a characteristic pulsation.

Let us now re-establish the magnetic drift velocity. It has mainly two consequences :

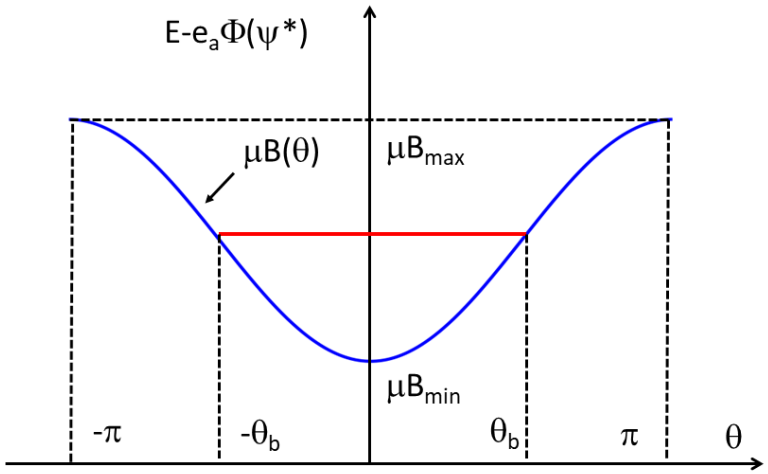

Figure 8: Magnetic well in a tokamak. A particle is passing if $E - e_a\phi(\psi_*) > \mu B_{max}$ since $u_\parallel$ never vanishes. A particle is trapped if $\mu B_{min} < E - e_a\phi(\psi_*) < \mu B_{max}$. It bounces at $\theta = \pm\theta_b$ where $u_\parallel = 0$

- the orbit width of guiding centre trajectories becomes finite. It can be conveniently calculated by using the invariance of the canonical toroidal momentum Eq.(10), i.e. $\psi = \psi_* + \frac{m_a}{e_a B(\psi_*,\theta)} I(\psi_*) u_\parallel$. One consequence of this relationship is that the displacement is dictated by the sign of the parallel velocity. For a trapped particle, both signs occur since the particle bounces back and forth. This produces a widening of the trajectory around the reference magnetic surface, which takes the typical form of a banana (see Fig.9). For passing particles, it rather corresponds to an horizontal shift of the trajectory with respect to the reference magnetic surface. The direction of this shift depends on the sign of the parallel velocity.

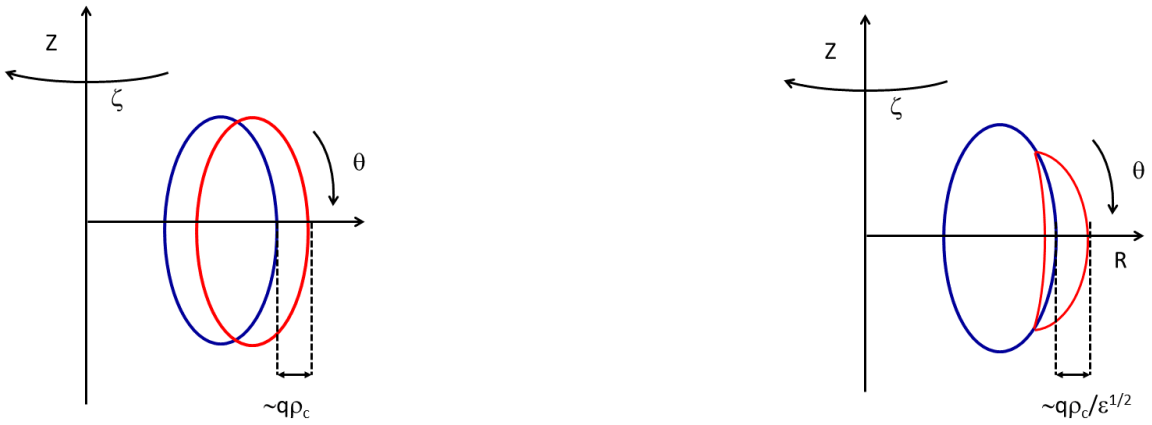

Figure 9: Poloidal cut of particle drift surfaces in a tokamak. Drift surfaces of passing particles are horizontally shifted by a distance $\sim q\rho_c$ (left panel). Trapped particles show a characteristic banana shape. The width is of the order of $\sim \frac{q\rho_c}{\sqrt{\epsilon}}$ (right panel). Banana tips are bounce points where the parallel velocity vanish.

- the guiding-centre toroidal angle is no longer determined by the condition $\zeta - q(\psi_*)\theta = \zeta_0$, i.e. the guiding centre does not strictly follow a field line any more. For trapped particles, this results in a slow precession motion with a characteristic pulsation Ω_d, called precession frequency. A similar process occurs for a passing particle, though sub-dominant compared with the quasi-uniform motion in ζ. Obviously the motion stays periodic.

This overall complex behaviour is characterized by 3 invariants of motions (E, μ, ψ_*), and 3 angles associated with 3 resonant pulsations. This is a case where the dynamical system is integrable, and trajectories are bounded, hence a system of angle/action variables can be derived. This set is built in the Appendix A and is summarized in the next section.

3.3.2 Angle/action variables in a tokamak

The equilibrium field is chosen to be up-down symmetric and described by the vector potential Eq.(6) that leads to the magnetic field

$$\mathbf{B} = I(\psi)\nabla\zeta + \nabla\zeta \times \nabla\psi = \nabla\left(\zeta - q(\psi)\theta\right) \times \nabla\psi$$

where ψ and $\chi(\psi)$ are the poloidal and toroidal fluxes normalised to 2π, ζ is the toroidal angle, and θ is a straight field line poloidal coordinate such that $\frac{\mathbf{B}\cdot\nabla\zeta}{\mathbf{B}\cdot\nabla\theta} = q(\psi)$, with $q(\psi)$ the safety factor. The Jacobian inverse of this set of coordinates is $\mathcal{J} = (\nabla\zeta \times \nabla\psi)\cdot\nabla\theta = \mathbf{B}\cdot\nabla\theta = I/qR^2$. Ignoring the electric potential, the link between the particle coordinates and the Hamiltonian angles is

$$\begin{aligned}
\psi &= -\frac{J_3}{e_a} + \hat{\psi}(\mathbf{J}, \alpha_b) \\
\theta &= \epsilon_c \alpha_b + \hat{\theta}(\mathbf{J}, \alpha_b) \\
\zeta &= \bar{\zeta} + q\left(-\frac{J_3}{e_a}\right)\hat{\theta}(\mathbf{J}, \alpha_b) + \widehat{\zeta}(\mathbf{J}, \alpha_b)
\end{aligned}$$

where

$$\hat{\theta}(\mathbf{J}, \alpha_b) = \frac{1}{\Omega_b}\int_0^{\alpha_b} d\alpha' \widetilde{\Omega}_\theta(\mathbf{J}, \alpha')$$

$$\widehat{\zeta}(\mathbf{J},\alpha_b) = \frac{1}{\Omega_b}\int_0^{\alpha_b} d\alpha' \widetilde{\Omega}_\alpha\left(\mathbf{J},\alpha'\right)$$

$$\hat{\psi}(\mathbf{J},\alpha_b) = \frac{m_a I u_\parallel}{e_a B}$$

are modulations, i.e. periodic functions of α_b with zero mean, $\tilde{F} = F - \langle F\rangle$ for any function F,

$$\Omega_\theta = \frac{\mathcal{J} u_\parallel}{B}$$

and

$$\Omega_\alpha = \frac{dq}{d\psi}\Omega_\theta\hat{\psi} + \mathbf{v}_D\cdot\nabla\zeta - q\mathbf{v}_D\cdot\nabla\theta$$

where the r.h.s. are to be calculated on the reference magnetic surface $\psi_* = -J_3/e_a$. The angular frequencies are

$$\begin{aligned}
\Omega^1(\mathbf{J}) &= \Omega_\varsigma(\mathbf{J}) = \langle\Omega_c\rangle \\
\Omega^2(\mathbf{J}) &= \Omega_b(\mathbf{J}) = \langle\Omega_\theta\rangle \\
\Omega^3(\mathbf{J}) &= \Omega_\zeta(\mathbf{J}) = \epsilon_c q\left(-\frac{J_3}{e_a}\right)\Omega_b(\mathbf{J}) + \Omega_d(\mathbf{J}) + e_a\frac{d\phi}{dJ_3}\left(-\frac{J_3}{e_a}\right)
\end{aligned}$$

where $\Omega_d = \langle\Omega_\alpha\rangle$, and $(\Omega_\varsigma,\Omega_b,\Omega_\zeta)$ are notations usually found in the literature, rather than $(\Omega^1,\Omega^2,\Omega^3)$. The bracket $\langle\rangle$ indicate an average over time $\int_{-\pi}^{\pi}\frac{d\alpha_b}{2\pi}F(\mathbf{J},\alpha_b)$, that can also be written as

$$\langle F\rangle(\mathbf{J}) = \Omega_b(\mathbf{J})\oint\frac{d\theta}{2\pi\Omega_\theta(\mathbf{J},\theta)}$$

where the integral has to be done over a one poloidal turn for passing particles, and a poloidal bounce interval for trapped particles. All primitive in α_b can be transformed into primitives in θ using the relation $\frac{d\alpha_b}{\Omega_b(\mathbf{J})} = \frac{d\theta}{\Omega_\theta(\mathbf{J},\theta)}$. This allows inverting the relations above and expressing the angles as function of the coordinates (θ,ζ) for a given set of invariants of motion $\mathbf{J}$. The actions are given by the relations

$$\begin{aligned}
J_1 &= \frac{m_a}{e_a}\mu \\
J_2 &= \epsilon_c e_a\chi\left(-\frac{J_3}{e_a}\right) + \oint\frac{d\ell}{2\pi}m_a u_\parallel \\
J_3 &= P_\zeta
\end{aligned}$$

where $\epsilon_c = 1$ (resp. 0) for passing (resp. trapped) particles, ℓ is the length element along field lines. This set of equations provides the correspondence between the actions $\mathbf{J}$ and the invariants of motion (E,μ,P_ζ) (plus the sign of the parallel velocity for passing particles). Explicit expressions of the quantities above can be computed in the special case of circular concentric magnetic surfaces (see Appendix B).

A set of angle/action variables is a powerful tool to demonstrate analytical results on various topics in plasma stability and turbulent transport. However it is not necessarily the best one for numerical applications, reason being the complexity of the change of variables from guiding-centre to angle/action variables. An alternative of course is to solve directly the set of guiding-centre equations of motion using the non-canonical variables $(\mathbf{X},u_\parallel)$. The various options are summarised in Fig.10.

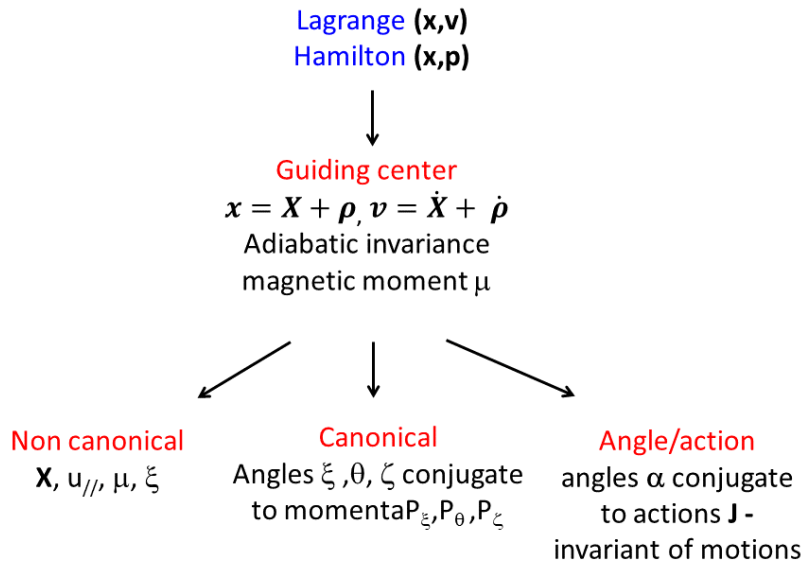

Figure 10: Choice of coordinates in a confining magnetic configuration.

Appendices

A Construction of a set of angle-action variables in a tokamak

The objective of this appendix is to construct a set of angle/action variables in a tokamak. The analysis is restricted to the limit of thin orbit width compared to the length scale of the confining magnetic field. The equilibrium is supposed to be up-down symmetric.

A.1 Equations of motion

A.1.1 Equation of motion of a guiding-centre

The equilibrium magnetic field in a tokamak can be written in a Clebsch form

$$\mathbf{B} = \nabla \left[\zeta - q(\psi)\theta\right] \times \nabla\psi$$

where ζ is a toroidal angle (minus the geometric angle here), and θ a straight field line poloidal angle, i.e. such that $\frac{\mathbf{B}\cdot\nabla\zeta}{\mathbf{B}\cdot\nabla\theta} = q(\psi)$ - q is the safety factor, and depends on ψ only (ψ is minus the poloidal flux normalised to 2π). The magnetic field derives from a vector potential

$$\mathbf{A} = \chi(\psi)\nabla\theta - \psi\nabla\zeta$$

where $\chi(\psi)$ is the flux of the toroidal field normalised to 2π - it verifies $\frac{d\chi}{d\psi} = q(\psi)$. An equivalent formulation of the field is

$$\mathbf{B} = I(\psi)\nabla\zeta + \nabla\zeta \times \nabla\psi$$

where I depends on ψ only (flux function). The field is the sum of a toroidal field $\mathbf{B}_T = I(\psi)\nabla\zeta$ and a poloidal field $\mathbf{B}_p = \nabla\zeta \times \nabla\psi$. The intensity of the poloidal field is usually smaller than its toroidal counterpart. This results in a total field intensity that

decreases with the major radius R since $|\nabla\zeta| = 1/R$.

The electric potential is ignored in a first step. It is shown in section A.5 that its main role is merely to modify the third angular pulsation. In absence of electric field, the equation of motion of a guiding-centre reduces to

$$\frac{d\mathbf{X}}{dt} = \dot{\mathbf{X}} = u_\parallel \mathbf{e}_\parallel + \mathbf{v}_D$$

where $\mathbf{e}_\parallel$ is the unit vector along the magnetic field computed at the guiding-centre position $\mathbf{X}$, and

$$\mathbf{v}_D = \frac{\mathbf{e}_\parallel}{e_a B^*_\parallel} \times \left(\mu \nabla B + m_a u_\parallel^2 \boldsymbol{\kappa} \right)$$

is the magnetic drift velocity, with $B^*_\parallel = \mathbf{e}_\parallel \cdot \mathbf{B}^* = B + \frac{m_a u_\parallel}{e_a} \mathbf{e}_\parallel \cdot \nabla \times \mathbf{e}_\parallel$ the Jacobian of the guiding-centre set of coordinates and $\boldsymbol{\kappa} = (\mathbf{e}_\parallel \cdot \nabla)\mathbf{e}_\parallel$ the field line curvature. The equation of motion for each coordinate $X^i = (\psi, \theta, \zeta)$ writes

$$\frac{dX^i}{dt} = \dot{\mathbf{X}} \cdot \nabla X^i = \dot{X}^i$$

It is recalled that the magnetic moment μ, kinetic energy $E = \frac{1}{2} m_a u_\parallel^2 + \mu B$, and canonical toroidal momentum $P_\zeta = -e_a \psi + m_a I u_\parallel / B$ are invariants of motion, where B and R are functions of (ψ, θ).

A.1.2 Approximation of thin orbit widths

The displacement of the guiding-centre position with respect to a reference magnetic surface is of the order of a gyroradius ρ_c normalised to the plasma size a, noted $\rho_* = \rho_c / a$ - a parameter small against 1 in fusion plasmas[19]. This can be demonstrated as follows. Les us introduce a reference magnetic surface $\psi = \psi_*$ such that $P_\zeta = -e\psi_*$, then

$$\psi = \psi_* + \frac{m_a I u_\parallel}{e_a B}$$

where ψ_* is an invariant of motion since it is proportional to P_ζ. It is also a label of a magnetic surface, that we denote here as "reference" magnetic surface. Defining an effective minor radius as $r = (2\chi/B_0)^{1/2}$, where B_0 is some reference constant magnetic field at a radius R_0 [20], and using $d\psi = B_0 r dr / q$, it is readily found that $r_G = \bar{r} + \frac{qR}{\bar{r}} \rho_\parallel + o(\rho_*^2)$, where $\rho_\parallel = \frac{u_\parallel}{\Omega_c}$ is a gyroradius built with the particle parallel velocity instead of its perpendicular component. Hence the transverse displacement with respect to the reference magnetic surface is of the order of a gyroradius, and therefore small compared with the plasma size. This is expected for a confining magnetic configuration. The normalised gyroradius also measures the ratio of the magnetic drift to the parallel velocity. This allows to proceed in two steps: first solve the fast parallel motion, then the slow magnetic drift. This procedure can be formalized as follows. The radial position of the particle guiding centre is written as $\psi = \psi_* + \hat{\psi}$, where $\hat{\psi} \ll \psi_*$. There is some flexibility in the choice of ψ_*. Throughout this note $P_\zeta = -e_a \psi_*$ is adopted - alternatives are discussed in section A.3.2. The equations of motion are then expanded at first order in ρ_*, i.e.

$$\frac{d\hat{\psi}}{dt} = \mathbf{v}_D \cdot \nabla \psi \tag{11}$$

$$\frac{d\theta}{dt} = \Omega_\theta|_{\mathbf{X}_*} + \left. \frac{d\Omega_\theta}{d\psi} \right|_{\mathbf{X}_*} \hat{\psi} + \mathbf{v}_D \cdot \nabla \theta \tag{12}$$

$$\frac{d\zeta}{dt} = q\Omega_\theta|_{\mathbf{X}_*} + \left. \frac{d}{d\psi} (q\Omega_\theta) \right|_{\mathbf{X}_*} \hat{\psi} + \mathbf{v}_D \cdot \nabla \zeta \tag{13}$$

[19] In fact the condition $\rho_* \ll 1$ defines a magnetised plasma.

[20] The flux of a constant axial field B_0 through a cylindrical surface of radius r is $\pi B_0 r^2$, i.e. $\chi = B_0 r^2/2$, so that r coincides with the usual definition of a minor radius for a set of circular concentric magnetic surfaces with large aspect ratio $R_0/r \gg 1$.

where $...|_{\mathbf{X}_*}$ means "calculated at $\mathbf{X} = \mathbf{X}_* = (\psi_*, \theta)$", Ω_θ is the poloidal particle transit pulsation

$$\Omega_\theta\left(E, \mu, \epsilon_\parallel, \psi, \theta\right) = \frac{\mathcal{J} u_\parallel}{B}$$

where $\epsilon_\parallel$ is the sign of the parallel velocity, and $\mathcal{J} = \mathbf{B} \cdot \nabla\theta = I/qR^2$ is the inverse Jacobian of the coordinate system (ψ, θ, ζ). Both $\mathcal{J}$ and B depend on (ψ, θ), while q depends on ψ only. The parallel velocity is a function of $(E, \mu, \epsilon_\parallel, \psi, \theta)$. In the following we will use the dimensionless invariant of motion $\lambda = \mu B_0/E$ instead of μ. The parallel velocity then writes

$$u_\parallel = \epsilon_\parallel \sqrt{\frac{2E}{m}} \sqrt{1 - \lambda b\left(\psi, \theta\right)}$$

where $b\left(\psi, \theta\right) = B\left(\psi, \theta\right)/B_0$[21]. To simplify the notations, the 3 invariants of motion (E, λ, ψ_*) are labelled as a vector $\mathbf{J}$, anticipating that 3 actions (J_1, J_2, J_3) exist and are functions of (E, λ, ψ_*). Furthermore, it is necessary to track down the sign $\epsilon_\parallel$ of the parallel velocity $u_\parallel$ for passing particles - this sign is implicitly included in the action vector $\mathbf{J}$. Each velocity component $\mathbf{v}_D \cdot \nabla x^i$ is computed as a function of $(\mathbf{J}, \theta)$ by just replacing everywhere ψ with ψ_*. Fields are now expressed as functions of $(\mathbf{J}, \theta)$.

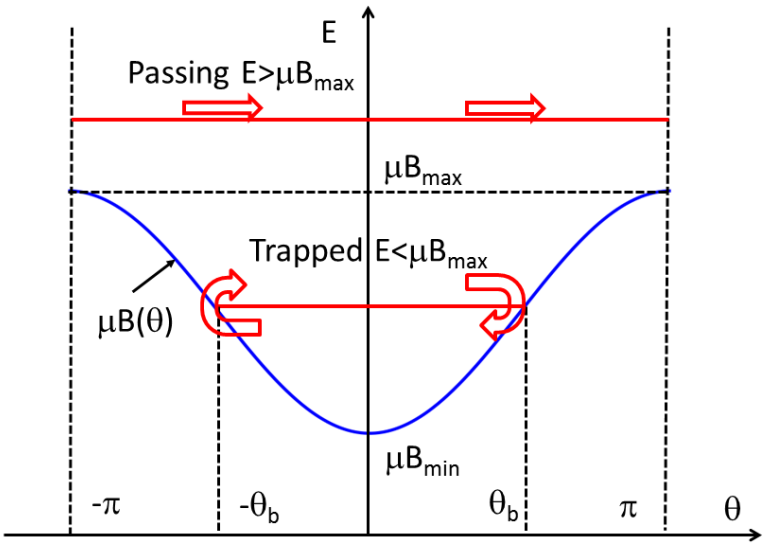

Figure 11: Parallel motion of a charged particle. If the energy E exceeds μB_{max}, the particle is passing and moves always in one direction only. If $E < \mu B_{max}$, the particle bounced back and is trapped in the magnetic well along the field lines.

A.2 Motion along the field lines

When ignoring the magnetic drift in Eq.(11), it appears that $\hat{\psi}$ is a constant, that we choose arbitrarily equal to zero. This implies that $\psi(t) = \psi_*$, i.e. the particle guiding-centre stays on the reference magnetic surface and follows a field line. Another choice would imply that the reference magnetic surface is not $\psi = \psi_*$, but another invariant of motion. This option is perfectly legitimate, and will be discussed in section A.3.2. The value of ψ_* is entirely determined by the canonical toroidal moment computed at

[21] In the standard ordering of a tokamak, this expression is not affected by the electric potential which scales as ρ_* compared with the kinetic energy - see section A.5.

$t = 0$. This also means that the toroidal angle is set by the condition $\zeta - q(\psi_*)\theta = \zeta_0$, the constant ζ_0 being prescribed by the initial conditions. It is then sufficient to determine the poloidal angle $\theta(t)$. Its evolution equation is given by Eq.(12) that becomes

$$\frac{d\theta}{dt} = \left.\frac{\mathcal{J}u_\parallel}{B}\right|_{\mathbf{X}_*} \Omega_\theta(\mathbf{J},\theta) \tag{14}$$

This equation describes an autonomous system in θ for a given set of invariants of motion. An autonomous system means that $\frac{d\theta}{dt}$ is a function of θ only for a fixed set of invariants and can be integrated as

$$t = \int^\theta \frac{d\theta'}{\Omega_\theta(\mathbf{J},\theta')} \tag{15}$$

where

$$\Omega_\theta(\mathbf{J},\theta) = \epsilon_\parallel \sqrt{\frac{2E}{m_a}} \left[1 - \lambda b\left(\psi_*,\theta\right)\right]^{1/2} \frac{\mathcal{J}\left(\psi_*,\theta\right)}{B\left(\psi_*,\theta\right)}$$

and $\epsilon_\parallel$ is the sign of the parallel velocity. Note that $d\theta/\Omega_\theta$ could as well be written $d\ell/u_\parallel$, where ℓ is the abscissa along the field line and satisfies $d\ell/B = d\theta/\mathbf{B}\cdot\nabla\theta$. Two cases occur. First the particle slows down due to the mirror force, reaches a point where its parallel velocity cancels, and finally bounces back. It is then called "trapped". In the second case, the particle moves forward (or backward) and does not bounce (see Fig. 11). It is dubbed "passing" or "circulating". In a tokamak the magnetic field exhibits a minimum $B_{min}(\psi_*)$ on a magnetic surface $\psi = \psi_*$ on the so-called "low field side" (we choose the coordinate origin $\theta = 0$ at this place), and a maximum $B_{max}(\psi_*)$ on the "high field side" (at $\theta = \pi$). A particle is trapped whenever $\lambda = \mu B_0/E$ ranges between B_0/B_{max} and B_0/B_{min}, while it is passing if $0 \leq \lambda \leq B_0/B_{max}$. The equation $1 - \lambda b\left(\psi_*,\theta_b\right) = 0$ defines the poloidal position $\theta_b(\mathbf{J})$ of the bounce point. The phase space (E,λ) is therefore split in two domains: trapped and passing. The trapped/passing boundary is determined by the line $\lambda = B_0/B_{max}$. If θ_b is a bounce point, then $-\theta_b$ is also a bounce point - a consequence of the assumption of up-down symmetric equilibrium - by convention θ_b is the positive root. This means that a trapped particle bounces between $-\theta_b$ and θ_b. A bounce point appears as an integrable singularity in the r.h.s. of the integral Eq.(15) since $\int^\theta d\theta/\sqrt{\theta_b - \theta}$ remains a regular function. We arrive now to an important point. For a given set of invariants of motion, the motion $\theta(t)$ is periodic in time, independently of the nature of the trajectory (trapped or passing), with a pulsation Ω_b and a period $T_b = 2\pi/\Omega_b$. This implies that θ and ζ can be expressed as periodic functions of the angular variable $\alpha_b = \Omega_b t + \alpha_{b0}$, where α_{b0} is set by the initial condition on θ. Hence one can use indistinctly the time t or the angular variable α_b to describe the motion. The angle α_b is nothing else than the second angle variable α^2. We investigate now this key point.

A.2.1 Second angle variable for a passing particle

For passing particles, the motion is 2π-periodic in θ. The period is the time needed to move from $\theta = -\pi$ to $\theta = \pi$ (the choice of the integration interval is arbitrary provided its length is 2π). The period is $2\pi/\Omega_b$, where $\Omega_b\left(\mathbf{J}\right)$ is the transit pulsation. Integrating Eq.(14), one gets the following relation

$$\frac{2\pi}{\Omega_b(\mathbf{J})} = \int_{-\pi}^{\pi} \frac{d\theta}{\Omega_\theta(\mathbf{J},\theta)}$$

The motion of the particle can be decomposed in a uniform motion in θ, plus a modulation[22]. A uniform motion means $\theta = \Omega_b t + \alpha_{b0}$, where α_{b0} is set by the initial condition at θ at $t = 0$. It is convenient to introduce an angle $\alpha_b = \Omega_b t + \alpha_{b0}$, such that $\theta = \alpha_b$ for

[22] A modulation is meant here as a periodic function with zero mean.

a uniform motion. This is a reasonable description of the motion for nearly freely passing particles $mu_{\|}^2/2 \gg \mu B$, but not appropriate near the passing/trapped boundary. It is thus necessary to compute the departure from a pure uniform motion, i.e. $\theta = \alpha_b + \hat{\theta}(\mathbf{J}, \alpha_b)$, where $\hat{\theta}(\mathbf{J}, \alpha_b)$ has to be a 2π-periodic function in α_b. Let us introduce a time average as

$$\langle F \rangle (\mathbf{J}) = \Omega_b(\mathbf{J}) \int_{-\pi}^{\pi} \frac{d\theta}{2\pi \Omega_\theta(\mathbf{J}, \theta)} F(\mathbf{J}, \theta)$$

for any function $F(\mathbf{J}, \theta)$ (note that $\langle F \rangle = 1$). Any function $F(\mathbf{J}, \theta)$ can then be split in its time average plus a modulation $\widetilde{F} = F - \langle F \rangle$, i.e. $F(\mathbf{J}, \theta) = \langle F \rangle (\mathbf{J}) + \widetilde{F}(\mathbf{J}, \theta)$, where $\widetilde{F}(\mathbf{J}, \theta)$ is a periodic function of θ , and hence of α_b, with zero mean. Hence

$$\frac{d\theta}{dt} = \langle \Omega_\theta \rangle (\mathbf{J}) + \widetilde{\Omega}_\theta(\mathbf{J}, \theta)$$

where $\langle \Omega_\theta \rangle = \Omega_b$. This provides the formal modulation

$$\hat{\theta}(\mathbf{J}, \theta) = \int_0^{\theta} \frac{d\theta'}{\Omega_\theta(\mathbf{J}, \theta')} \widetilde{\Omega}_\theta(\mathbf{J}, \theta') \tag{16}$$

which has to be a periodic function of α_b since it is the primitive in α_b of a periodic function in α_b with zero mean. A zero lower bound is chosen, which grants that θ is an odd function of α_b (other choices are possible). Eq.(16) sets an implicit equation on the link between θ and α_b, i.e. $\theta - \hat{\theta}(\mathbf{J}, \theta) = \alpha_b$. This relation can be inverted to get the formal solution

$$\theta = \alpha_b + \hat{\theta}(\mathbf{J}, \alpha_b)$$

where $\hat{\theta}(\mathbf{J}, \alpha_b)$ is a periodic modulation of α_b. Hence α_b is an angular variable that describes the motion of passing particles, and can be identified as the second angle α^2, while Ω_b is the second angular pulsation Ω^2.

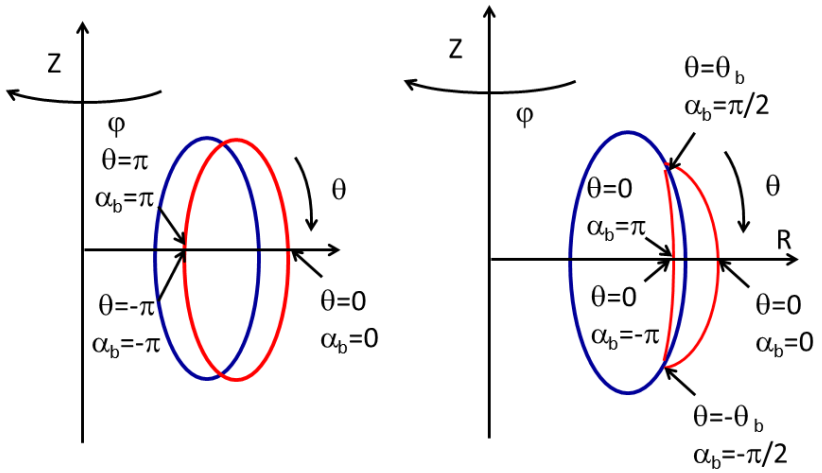

Figure 12: Values of the angle variable α_b at peculiar positions of a particle trajectory - a) left panel: passing particle b) right panel trapped particle.

α_b	$-\pi$	$-\frac{\pi}{2}$	0	$\frac{\pi}{2}$	π
θ	0	$-\theta_b$	0	θ_b	0
$\frac{d\theta}{d\alpha_b}$	$-$	0	$+$	0	$-$
$u_\parallel$	$-$	0	$+$	0	$-$

Table 1: Variations of poloidal angles and bounce angular variable during a bounce period.

A.2.2 Second angle variable for a trapped particle

The motion of a trapped particle is far from uniform since the particle bounces back and forth between the turning points $\pm\theta_b(\mathbf{J},\alpha_b)$. The period of the motion of a trapped particle is the time needed to move from the bounce point $-\theta_b$ to θ_b, and then back to θ_b. The period is again $2\pi/\Omega_b$, where Ω_b is the bounce pulsation. The easiest way is to compute a half-period, i.e.

$$\frac{\pi}{\Omega_b(\mathbf{J})} = \int_{-\theta_b}^{\theta_b} \frac{d\theta}{|\Omega_\theta(\mathbf{J},\theta)|}$$

Note that Ω_b is positive, in contrast with passing particles, for which Ω_b keeps the sign of the parallel velocity. For trapped particles, the bounce motion incorporates both positive and negative parallel velocities. As for passing particles, a time average can be constructed, which requires some care. The safest way to define an average of a function $F(E,\mu,\psi_*,\epsilon_\parallel,\theta)$ is to involve a time average $\langle F\rangle = \frac{1}{T_b}\int_0^{T_b} dt F(E,\mu,\psi_*,\epsilon_\parallel,\theta(t))$, which can be conveniently recast as an integral over the poloidal angle

$$\langle F\rangle = \frac{2\pi}{\Omega_b}\int_{-\theta_b}^{\theta_b} \frac{d\theta}{|\Omega_\theta(\mathbf{J},\theta)|}\left[F(E,\mu,\psi_*,\epsilon_\parallel,\theta)+F(E,\mu,\psi_*,-\epsilon_\parallel,\theta)\right]$$

Note that the parallel velocity is positive on the way from $-\theta_b$ to θ_b, assuming a positive Jacobian. It appears that the average of an odd function in parallel velocity is zero. The poloidal angle θ is a function $\hat{\theta}(\mathbf{J},\alpha_b)$, periodic in α_b, where $\alpha_b = \Omega_b t + \alpha_{b0}$, and α_{b0} is set by the initial condition on θ at $t=0$. The implicit expression of $\hat{\theta}$ is given by Eq.(15). To make the picture more precise, let us construct the explicit link between α_b and θ over the different phases of the bounce motion when imposing that θ is an odd function of α_b

$$\begin{array}{ccc} -\pi \le \alpha_b \le -\frac{\pi}{2} & ; & \alpha_b = -\frac{\pi}{2} - \Omega_b \int_{-\theta_b}^{\theta} \frac{d\theta'}{|\Omega_\theta(\mathbf{J},\theta')|} \\ -\frac{\pi}{2} \le \alpha_b \le \frac{\pi}{2} & ; & \alpha_b = -\frac{\pi}{2} + \Omega_b \int_{-\theta_b}^{\theta} \frac{d\theta'}{|\Omega_\theta(\mathbf{J},\theta')|} \\ \frac{\pi}{2} \le \alpha_b \le \pi & ; & \alpha_b = \frac{3\pi}{2} - \Omega_b \int_{-\theta_b}^{\theta} \frac{d\theta'}{|\Omega_\theta(\mathbf{J},\theta')|} \end{array}$$

The variations are summarised in table 1 and in Fig. 12. A convenient alternative expression of the average of a function with zero mean is just $\langle F\rangle = \int_{-\pi}^{\pi} \frac{d\alpha_b}{2\pi} F(\mathbf{J},\alpha_b)$, where the choice of the lower and upper bounds in the integral does not matter as long as they differ by 2π.

A.3 Effect of the magnetic drift

A.3.1 Orbit width and toroidal motion

When re-establishing the magnetic drift in the set of equations of motion Eqs.(11-13), three modifications emerge:

- the orbit width of guiding centre trajectories, measured by the excursion $\hat{\psi}$, is finite.

- the poloidal angle is modified. It is decomposed as $\theta(\mathbf{J},\alpha_b) = \theta^{(0)}(\mathbf{J},\alpha_b) + \theta^{(1)}(\mathbf{J},\alpha_b)$, where $\theta^{(0)}(\mathbf{J},\alpha_b)$ is the trajectory computed in section A.2 (fast motion along the

field lines), while $\theta^{(1)}(\mathbf{J},\alpha_b)$ is the modification due to the magnetic drift. This corresponds to an expansion in ρ_*. Both functions are periodic in α_b.

- the toroidal angle is no longer determined by the condition $\zeta - q(\psi_*)\theta = \zeta_0$, i.e. the guiding centre does not strictly follow a field line any more.

Let us detail these points. The finite orbit width $\hat{\psi}$ is dictated by Eq.(11), where the right hand side must be calculated at $\psi = \psi_*$, and $\theta = \theta^{(0)}(\mathbf{J},\alpha_b)$. The higher order correction $\theta^{(1)}(\mathbf{J},\alpha_b)$ introduces $o(\rho_*^2)$ corrections to $\hat{\psi}$. However it would be unproductive to resolve the evolution equation that dictates $\hat{\psi}$. It is much more efficient to use the invariance of the canonical toroidal momentum, which gives immediately $\hat{\psi} = \frac{m_a I u_\parallel}{e_a B}$. Given the expansion ordering, the right hand side must be calculated at $\psi = \psi_*$, and $\theta = \theta^{(0)}$.

The poloidal angle θ is slightly modified by the poloidal projection of the magnetic drift and the finite orbit width, as evidenced by Eq.(12), i.e. $d\theta^{(1)}/dt = (d\Omega_\theta/d\psi)\hat{\psi} + \mathbf{v}_D \cdot \nabla\theta$, where the right hand side is calculated at $\psi = \psi_*, \theta = \theta^{(0)}$. This correction is small (ρ_* is a few 10^{-3} in a fusion plasma), and can be ignored in most practical applications.

The effect of the magnetic drift on the toroidal angle can be assessed a follows. To isolate the slow motion due to the magnetic drift from the fast parallel motion, it is convenient to introduce the variable $\bar{\alpha} = \zeta - q(\psi_*)\theta^{(0)}$. Combining Eqs.(12,13), it appears that

$$\frac{d\bar{\alpha}}{dt} = \Omega_\alpha\left(\mathbf{J},\theta\right) \tag{17}$$

where

$$\Omega_\alpha\left(\mathbf{J},\theta\right) = \frac{dq}{d\psi}\Omega_\theta\hat{\psi} + \mathbf{v}_D \cdot \nabla\zeta - q\mathbf{v}_D \cdot \nabla\theta$$

All quantities on the *r.h.s.* of Eq.(18) must be calculated at $\psi = \psi_*, \theta = \theta^{(0)}$. It appears that the motion in $\bar{\alpha}$ is slow since it involves the magnetic drift only, so $o(\rho_*)$. The magnetic drift pulsation Ω_α can be decomposed into a time average (in fact better seen as an average over the angle α_b) and a modulation, i.e. $\Omega_\alpha = \langle\Omega_\alpha\rangle + \widetilde{\Omega}_\alpha$. Conventionally, the average pulsation $\langle\Omega_\alpha\rangle$ due to the magnetic drift is noted Ω_d - it is a function of the invariants of motion only. An integration in time gives $\bar{\alpha}(t) = \Omega_d(\mathbf{J})t + \widehat{\zeta}(\mathbf{J},t)$, where $\widehat{\zeta}(\mathbf{J},t) = \int^t dt'\widetilde{\Omega}_\alpha\left(\mathbf{J},\theta(t')\right)$. The key point is that $\widehat{\zeta}(\mathbf{J},t)$ can also be written as a periodic function of α_b since it is the primitive of a function $\widetilde{\Omega}_\alpha\left(\mathbf{J},\alpha_b\right)$, periodic in α_b with zero mean. The function $\widetilde{\Omega}_\alpha\left(\mathbf{J},\alpha_b\right)$ is computed from $\widetilde{\Omega}_\alpha\left(\mathbf{J},\theta\right)$ by expressing θ as a periodic function of α_b. After a reorganisation of the various terms, the toroidal angle appears to be

$$\zeta = \bar{\zeta} + q\left(\psi_*\right)\hat{\theta}(\mathbf{J},\alpha_b) + \widehat{\zeta}(\mathbf{J},\alpha_b) \tag{18}$$

where $\bar{\zeta} = \Omega_\varphi t + \bar{\zeta}_0$,

$$\Omega_\varphi(\mathbf{J}) = \Omega_d(\mathbf{J}) + q\left(\psi_*\right)\epsilon_c\Omega_b(\mathbf{J})$$

with $\epsilon_c = 1$ (resp. 0) for passing (resp. trapped particles), and

$$\widehat{\zeta}(\mathbf{J},\alpha_b) = \frac{1}{\Omega_b}\int_0^{\alpha_b} d\alpha'\widetilde{\Omega}_\alpha\left(\mathbf{J},\alpha'\right)$$

The constant $\bar{\zeta}_0$ is determined by the initial condition on ζ. The expression Eq.(18) is the requested result. Indeed it can be seen as a change of coordinates that gives ζ as a function of invariants of motion and periodic in the angles α_b and $\bar{\zeta}$. Hence the angle $\bar{\zeta}$ is nothing else than the third angle variable α^3 and Ω_φ the third angular pulsation Ω^3.

A.3.2 Some remarks

Particle orbit width

The change of topology of the trajectories due to the shift $\hat{\psi} = \frac{m_a I u_\parallel}{e_a B}$ is not the same

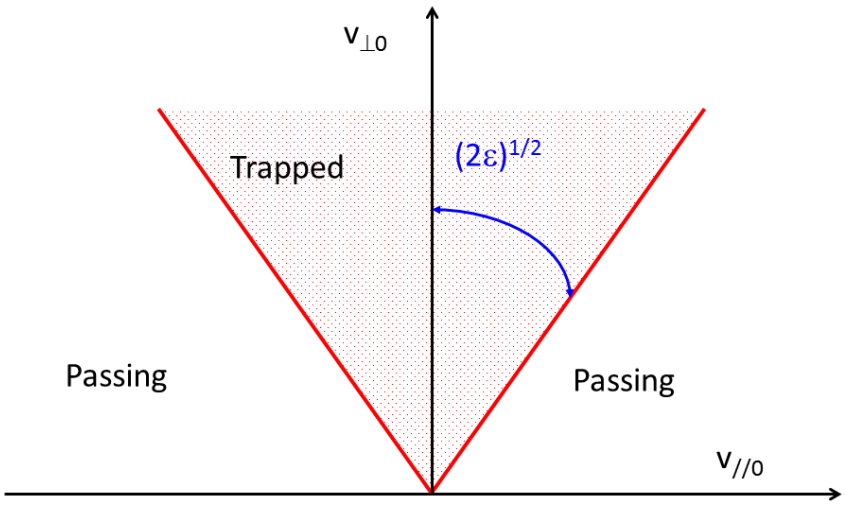

Figure 13: Domain of trapped particles in the phase space. $v_{\|0}$ is the parallel velocity at $\theta = 0$ and $\psi = \psi_*$ (low field side, equatorial plane) , $\epsilon = (B_{max} - B_{min})/B_0$ is the depth of the magnetic field well, $v_{\perp 0} = \sqrt{2\mu B_0/m_a}$ is the perpendicular velocity for the mean-magnetic field $B_0 = (B_{min} + B_{max})/2$.

for passing and trapped particles. Let us consider the case of a freely passing particle $1/2 m_a u_\|^2 \gg \mu B$. The parallel velocity is nearly a constant of motion since $E = 1/2 m_a u_\|^2$ is invariant. Let us remember that the field B behaves as $1/R$. This means that $\hat{\psi}$ behaves as $R(\psi_*, \theta)$, which mainly corresponds to an horizontal shift of the drift surface compared with the magnetic surface[23]. The horizontal shift is of the order of $q\rho_c$, using the same estimate as in section A.1.2 $d\psi/dr \sim I$. For trapped particles, $u_\|$ is a periodic function of time. A quantitative condition for trapping can be obtained with the following argument. The bounce point $u_\| = 0$ of a particle just at the trapped/passing boundary is located at $\theta = \pi$ where $B(\psi_*, \theta) = B_{max}$ (high field side). Calling $v_{\|0}$ the parallel velocity at $\theta = 0$ and $\psi = \psi_*$, energy conservation imposes that $\frac{1}{2} m_a v_{\|0}^2 + \mu B_{min} = \mu B_{max}$. Hence trapping occurs if $\left|u_\|\right| \leq v_{\|0}$, where $v_{\|0} = \sqrt{2\epsilon} v_{\perp 0}$, $2\epsilon = (B_{max} - B_{min})/B_0$ measures the depth of the magnetic field well, and $v_{\perp 0} = \sqrt{2\mu B_0/m_a}$ is the perpendicular velocity for the mean magnetic field $B_0 = (B_{min} + B_{max})/2$. This conditions draws a cone in the phase space $(v_{\|0}, v_{\perp 0}, \varsigma)$ - see Fig.13. Hence the fraction of trapped particles scales as $\sqrt{2\epsilon}$. Moreover an order of the displacement $\hat{\psi}$ is $q\rho_c/\epsilon^{1/2}$. The shape of the trajectory looks like a "banana", hence the common name "banana trajectory". The bounce points are called banana tips. Of course the shape of a trajectory changes continuously when moving in the variable $\lambda = \mu B_0/E$ from passing to trapped domain in the phase space. One important consequence of the relation $\hat{\psi} = \frac{m_a I u_\|}{e_a B}$ is a tight link between the sign of the parallel velocity and the radial displacement $\hat{\psi}$. Schematic shapes of passing and trapped particle trajectories are shown on Fig.15.

3rd resonant pulsation

There is a substantial difference between passing and trapped particles regarding the effect of the magnetic drift on the toroidal motion. The relation $\Omega_\varphi(\mathbf{J}) = q(\psi_*)\epsilon_c \Omega_b(\mathbf{J}) + \Omega_d(\mathbf{J})$

[23]the reader may convince himself by considering for instance a circular elliptic shape of magnetic surfaces $\psi \sim (R - R_0)^2 + Z^2$.

implies that for passing particles $\epsilon_c = 1$, the pulsation Ω_d is a correction to the contribution of the fast parallel motion $q\epsilon_c\Omega_b$ to the third angular pulsation Ω_φ. However for trapped particles $\epsilon_c = 0$, $\Omega_\varphi = \Omega_d$ so that the magnetic drift bring the major contribution to the third angular frequencies. The expression Eq.(18) of $\zeta(t)$ can be interpreted as follows. The toroidal motion of a trapped particle is the sum of a fast bounce motion along the field line $q\hat{\theta}$, plus a slow regular precession motion $\bar{\zeta} = \Omega_\varphi t + \bar{\zeta}_0$. The residue $\widehat{\zeta}$ indicates that the precession motion is not uniform in time. The pulsation Ω_d is called precession pulsation (or frequency).

Choice of the reference magnetic surface

The choice of the reference magnetic surface ψ_* matters for practical calculations. It has been chosen so far as $\psi_* = -P_\zeta/e_a$ to relate directly the reference surface with the canonical toroidal momentum. However this may not be an optimum choice. In principle any other choice ψ'_* is acceptable provided that is not too far away from the first one (within a few gyroradius). However it must be kept in mind that the pulsation Ω_d must be modified accordingly for passing particles. Indeed the pulsation Ω_d can be written differently by using $\frac{d\hat{\psi}}{dt} = \mathbf{v}_D \cdot \nabla\psi$, and $\frac{d\theta}{dt} = \Omega_\theta$. After an integration by parts

$$\Omega_d = \frac{1}{T_b}\frac{dq}{d\psi}\left[\theta\hat{\psi}\right]_0^{T_b} + \langle \mathbf{v}_D \cdot \nabla\alpha \rangle$$

where $\alpha = \zeta - q(\psi)\theta$ (note that α differs from $\bar{\alpha} = \zeta - q(\psi_*)\theta^{(0)}$). For trapped particles the first term cancels since the particle is back at the same poloidal angle after a period T_b. Hence $\Omega_d = \langle \mathbf{v}_D \cdot \nabla\alpha \rangle$ for trapped particles. This is not true for a passing particles since the poloidal angle has spanned 2π after a period. Using that $\hat{\psi}(T_b) = \hat{\psi}(0)$ (periodic motion) then

$$\Omega_d = \Omega_b \frac{dq}{d\psi}\hat{\psi}(T_b) + \langle \mathbf{v}_D \cdot \nabla\alpha \rangle$$

There is some degree of arbitrariness in the choice of $\hat{\psi}(T_b)$. We note however that it never vanishes for a reference surface ψ_* since in this case $\hat{\psi} = \frac{m_a I u_\parallel}{e_a B}$ and $u_\parallel$ differs from zero for passing particles. Of course the position of the guiding-centre must be left invariant by this change of reference magnetic surface, so that $\psi = \psi_* + \hat{\psi} = \psi'_* + \hat{\psi}'$. This implies that the new drift pulsation is related to the old one via the relation

$$\Omega'_d = \Omega_d - \Omega_b \frac{dq}{d\psi}\left(\psi'_* - \psi_*\right)$$

A important point is that the third angular pulsation $\Omega_\varphi = q(\psi_*)\Omega_b + \Omega_d = q(\psi'_*)\Omega_b + \Omega'_d$ is left invariant by this modification. In other words, the drift pulsation is changed, but this change is compensated by the change of transit pulsation $q(\psi_*)\Omega_b$. This is of course a reassuring result: the angular pulsation does not depend on a particular choice of reference magnetic surface. This conclusion holds for trapped particles.

The choice of ψ_* is not a wise choice for energetic particles since ψ_* may actually be far away from the drift surface. Another common choice is to choose the reference magnetic surface as the time average $\langle\psi\rangle_t$ of the particle, that is noted $\bar{\psi}$. Since P_ζ is an invariant of motion, it must be equal to its time average, which implies

$$P_\zeta = -e_a\psi_* = -e_a\psi + m_a\frac{Iu_\parallel}{B} = -e_a\bar{\psi} + m_a\left\langle\frac{Iu_\parallel}{B}\right\rangle_t$$

The time average of $\frac{Iu_\parallel}{B}$ can be calculated and leads to the following relationship

$$\bar{\psi} = \psi_* + m_a I(\psi_*)\Omega_b(\mathbf{J})\int_{-\pi}^{\pi}\frac{d\theta}{2\pi}\frac{1}{\mathbf{B}\cdot\nabla\theta}$$

which relates $\bar{\psi}$ and ψ_*. The derivation above also implies that the position of the guiding-centre

$$\psi = \bar{\psi} + \frac{m_a}{e_a}\left(\frac{Iu_\parallel}{B} - \left\langle \frac{Iu_\parallel}{B} \right\rangle_t\right)$$

stays close to the reference magnetic surface $\bar{\psi}$, even for passing particles. Alternatives choices to ψ_* or $\bar{\psi}$ are possible for the third invariant of motion. For instance the intersection of the trajectory with the equatorial plane is a possibility (a choice has to be made for trapped particles since the particle crosses twice the equatorial plane during a period). It allows performing local Taylor developments near this position. Another choice, not always possible, is a location where $\hat{\psi} = 0$. If the corresponding time is chosen as the initial time then $\hat{\psi}(0) = \hat{\psi}(T_b) = 0$, and the precession pulsation is given by the same relation as trapped particles $\Omega_d = \langle \mathbf{v}_D \cdot \nabla\alpha \rangle$.

First angle variable and resonant pulsation

The attentive reader may wonder about the fate of the cyclotron motion, and the first angular variable α^1. The equation of motion over the cyclotron angle is $\frac{d\varsigma}{dt} = \Omega_c(\mathbf{X})$. The right hand side can also be split into an average over the variable α_b plus a modulation $\Omega_c = \langle\Omega_c\rangle(\mathbf{J}) + \widetilde{\Omega}_c(\mathbf{J}, \alpha_b)$. It then appears that $\varsigma = \alpha^1 + \hat{\varsigma}(\mathbf{J}, \alpha_b)$, where

$$\hat{\varsigma}(\mathbf{J}, \alpha_b) = \frac{1}{\Omega_b}\int_0^{\alpha_b} d\alpha' \widetilde{\Omega}_c(\mathbf{J}, \alpha')$$

is a periodic function of α_b, and $\varsigma = \langle\Omega_c\rangle t + \varsigma_0$, where ς_0 is set by the initial conditions. The cyclotron angle ς can then be identified as the first angle α^1, and the average cyclotron pulsation $\langle\Omega_c\rangle$ as the first angular pulsation Ω^1. This final step full establishes a complete set of 3 angular variables and 3 invariants of motion.

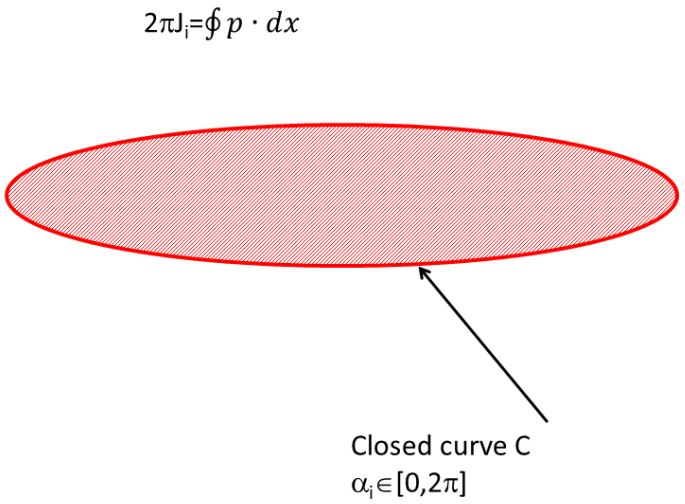

Figure 14: Calculation of an action via the integration of the canonical momentum on a closed curve.

A.4 Construction of the action variables

So far we have built a set of 3 angle variables $\boldsymbol{\alpha} = (\varsigma, \alpha_b, \bar{\zeta})$, associated with 3 invariants of motion $(E, \mu, P_\zeta = -e\psi_*)$. However these 3 invariants of motion are nor necessarily

actions in the usual definition, i.e. are not conjugate to the angles. Most calculations can be done without knowing the action variables, but it is nevertheless useful to know their expressions. This section aims at deriving them. There is no systematic recipe to construct an action, while knowing the trajectories. However one fast and efficient useful way is to make use of the following property: for any canonical change of coordinates, say from $(\mathbf{x}, \mathbf{p})$ to $(\bar{\mathbf{x}}, \bar{\mathbf{p}})$, the identity $\oint_{\mathcal{C}} \mathbf{p} \cdot d\mathbf{x} = \oint_{\mathcal{C}} \bar{\mathbf{p}} \cdot d\bar{\mathbf{x}}$ holds, where the integrals are performed over a closed contour $\mathcal{C}$. A set of angle/action variables $(\boldsymbol{\alpha}, \mathbf{J})$ is one particular example of canonical variables. Let us then build a closed contour in the phase space as the set of points $\mathbf{x}(\boldsymbol{\alpha}, \mathbf{J}), \mathbf{p}(\boldsymbol{\alpha}, \mathbf{J})$ where α^i spans $[0, 2\pi]$, all other α^k's constant and $\mathbf{J}$ constant, then $2\pi J_i = \oint_{\mathcal{C}} \mathbf{p} \cdot d\mathbf{x}$ (see Fig.14).

A.4.1 First action variable

Let us first use this recipe with $\alpha^1 = \varsigma$. The closed contour is then a cyclotron motion, at fixed guiding centre position. Using $\mathbf{p} = m_a \mathbf{v} + e_a \mathbf{A}$, it appears that $2\pi J_1 = \oint_{\mathcal{C}} m_a \mathbf{v}_c \cdot d\boldsymbol{\rho}_0 + e_a \oint_{\mathcal{C}} \mathbf{A} \cdot d\boldsymbol{\rho}_0$, where $\boldsymbol{\rho}_0$ is the cyclotron displacement, and $\mathbf{v}_c$ its velocity given by

$$\begin{aligned} \boldsymbol{\rho}_0(t) &= \rho_c \left(\cos\varsigma \mathbf{e}_1 - \sin\varsigma \mathbf{e}_2\right) \\ \mathbf{v}_c(t) &= v_\perp \left(-\sin\varsigma \mathbf{e}_1 - \cos\varsigma \mathbf{e}_2\right) \end{aligned}$$

Hence the first bit $\oint_{\mathcal{C}} m\mathbf{v}_c(t) \cdot d\boldsymbol{\rho}_0$ is equal to $2\pi m_a v_\perp^2 / \Omega_c$. The second piece is $e \oint_{\mathcal{C}} \mathbf{A} \cdot d\mathbf{x} = e \int_{\mathcal{S}} \mathbf{B} \cdot d^2\mathbf{x} = -\pi \rho_c^2$ [24]. Adding both contributions leads to $J_1 = \frac{m_a}{e_a}\mu$, an expected result [25].

A.4.2 Second action variable

Les us a consider a contour where α_b spans the interval $[0, 2\pi]$. This translates into a closed contour in the poloidal plane bounded by a drift surface. This drift surface is shifted with respect to the reference magnetic surface $\psi = \psi_*$. The action J_2 is split in two parts $J_2 = J_2^{(0)} + J_2^{(1)}$, where

$$\begin{aligned} J_2^{(0)} &= \oint_{\mathcal{C}} e_a \mathbf{A} \cdot \frac{d\mathbf{x}}{2\pi} \\ J_2^{(1)} &= \oint_{\mathcal{C}} m_a \mathbf{v} \cdot \frac{d\mathbf{x}}{2\pi} \end{aligned}$$

It is recalled that the vector potential is $\mathbf{A} = \chi \nabla\theta - \psi \nabla\zeta$, hence the first piece is

$$J_2^{(0)} = e_a \oint_{\mathcal{C}} \mathbf{A} \cdot \frac{d\mathbf{x}}{2\pi} = e_a \oint \frac{d\theta}{2\pi} \chi(\psi)$$

where $\psi = \psi_* + m_a I u_\parallel / e_a B$. Using $d\chi/d\psi = q(\psi)$, one gets

$$J_2^{(0)} = \epsilon_c e_a \chi(\psi_*) + \oint \frac{d\theta}{2\pi} \frac{qI}{B} m_a u_\parallel$$

The switch ϵ_c appears because of the different topology of trapped and passing trajectories. A trapped particle $\epsilon_c = 0$ bounces back and forth, so that in absence of magnetic drift $\psi = \psi_*$, the total toroidal flux enclosed by the trajectory is zero. This is not the case for

[24] The minus sign appears because the normal direction of the surface $\mathcal{S}$ enclosed by the contour is opposite to $\mathbf{B}$.

[25] A hasty judgement may lead the reader to consider this derivation as a fast demonstration of the adiabatic invariance of the magnetic moment μ. This is not the case: this whole section relies on equations of motion of guiding-centre variables which are based on adiabatic invariance. Nevertheless, a general theorem [5] does demonstrate that $\oint_{\mathcal{C}} \mathbf{p} \cdot d\mathbf{x}$ is conserved when conditions for adiabatic invariance apply.

a passing particle that turns around the magnetic axis (see Fig.15). Using the expression $\mathcal{J} = I/(qBR^2)$, an alternative expression of $J_2^{(0)}$ is

$$J_2^{(0)} = \epsilon_c e_a \chi(\psi_*) + \oint \frac{d\theta}{2\pi} \frac{|\mathbf{B}_T|^2}{\mathcal{J}B} m_a \; upar$$

where $\mathbf{B}_T = I\nabla\zeta$ is the toroidal field. The integrand has to be calculated at $\psi = \psi_*$, i.e. on the reference magnetic surface since it is $o(\rho_*)$. The second piece $J_2^{(1)}$ is also of order ρ_*, so calculated as well on the magnetic surface $\psi = \psi_*$ with $\mathbf{v} = u_\parallel \mathbf{e}_\parallel$. The length element vector is $d\mathbf{x} = \frac{d\theta}{\mathcal{J}} \mathbf{B}_p$, where $\mathbf{B}_p = \nabla\zeta \times \nabla\psi$ is the poloidal field, so that

$$J_2^{(1)} = \oint \frac{d\theta}{2\pi} \frac{m_a u_\parallel}{\mathcal{J}B} |\mathbf{B}_p|^2$$

Adding the two contributions provide the final expression of the second action

$$J_2 = \epsilon_c e_a \chi(\psi_*) + \oint \frac{d\ell}{2\pi} m_a u_\parallel$$

where $d\ell = d\theta \frac{B}{\mathcal{J}}$ is the length element along a field line. This action can be written in a somewhat more explicit form

$$J_2\left(E, \mu, \psi_*, \epsilon_\parallel\right) = \epsilon_c e_a \chi(\psi_*) + \epsilon_\parallel \oint \frac{d\theta}{2\pi} \frac{B}{\mathcal{J}} \sqrt{2m_a \left[E - \mu B\left(\psi_*, \theta\right)\right]}$$

It was seen that the magnetic moment is related to the first action, i.e. $\mu = \frac{e_a}{m_a} J_1$, and it will be seen in the next section that $\psi_* = -J_3/e_a$. Hence J_2 appears here as a function of the Hamiltonian $H_{eq} = E$ and the two other actions. One must have $\left.\frac{\partial J_2}{\partial J_1}\right|_{J_2,J_3} = 0$. Using the usual rules of chain derivatives, this implies that

$$\left.\frac{\partial J_2}{\partial E}\right|_{\mu,\psi_*} \Omega^1 + \frac{e_a}{m_a} \left.\frac{\partial J_2}{\partial \mu}\right|_{E,\psi_*} = 0$$

It is then recovered that $\Omega^1 = \langle \Omega_c \rangle$. In the same way, the constraint $\left.\frac{\partial J_2}{\partial J_3}\right|_{J_1,J_2} = 0$ implies

$$\Omega_\varphi = \Omega_b \frac{1}{e_a} \left.\frac{\partial J_2}{\partial \psi_*}\right|_{E,\mu}$$

In the case of trapped particles, the second invariant reduces to the "parallel adiabatic invariant" $J_2 = J_\parallel = \oint \frac{d\ell}{2\pi} m_a u_\parallel$.

A.4.3 Third action variable

Following the same approach with the angle $\bar{\zeta}$, it appears that the contour is now a circle of major radius R, since Eq.(18) imposes that if $\bar{\zeta}$ spans the interval $[0, 2\pi]$ then ζ also spans the interval $[0, 2\pi]$. The contour element is $d\mathbf{x} = R^2 \nabla\zeta d\zeta$, while $P_\zeta = e_a A_\varphi + m_a v_\varphi$ is an invariant of motion. As a result, the third action is just the canonical toroidal momentum $J_3 = P_\zeta = -e_a \psi_*$.

A.5 Effect of an electric potential

The primary effect of an electric potential is to add an $E \times B$ drift velocity to the guiding-centre perpendicular velocity. In the core of a fusion device, the electric potential is close to a flux function $\phi(\psi)$. Moreover the ion force balance equation in absence of strong flows implies that the ion thermal pressure gradient balances the electric force and therefore that $\phi \sim T_i/e_i$, where T_i is the ion temperature. It then appears that the drift frequency

Figure 15: Poloidal cut of particle drift surfaces in a tokamak. Drift surfaces of passing particles are horizontally shifted by a distance $\sim q\rho_c$ (left panel). The flux of the toroidal field is close to the reference magnetic flux. Trapped particles show a characteristic banana shape. The width is of the order of $\sim \frac{q\rho_c}{\sqrt{\epsilon}}$ (right panel). Banana tips are bounce points where the parallel velocity vanish. The flux of the toroidal field is small and vanishes in the limit of small magnetic drift.

is quite small compared with the ion cyclotron frequency, i.e. $v_E/a \sim \rho_*^2\Omega_c$. Hence the bounce motion is weakly affected by the $E \times B$ drift velocity. The third angular pulsation is modified though. Indeed the evolution equation of $\bar{\alpha} = \zeta - q(\psi_*)\theta^{(0)}$ Eq.(17) has its right hand side modified. The pulsation Eq.(18) is shifted by

$$\delta\Omega_\alpha\left(\mathbf{J},\theta\right) = \mathbf{v}_E \cdot \nabla\zeta - q(\psi_*)\mathbf{v}_E \cdot \nabla\theta$$

where it is reminded that $\mathbf{v}_E = \frac{1}{B_{||}^*}\mathbf{e}_{||} \times \nabla\phi$. Because of the ρ_* scaling adopted for $\phi(\psi)$, $B_{||}^*$ can be replaced by B, and ψ by ψ_*. The pulsation shift then reads $\delta\Omega_\alpha\left(\mathbf{J},\theta\right) = -\frac{d\phi}{d\psi_*}$. Hence the third pulsation is shifted by $-\frac{d\phi}{d\psi_*}$. This result can be obtained in a much faster way by noting that the Hamiltonian is $H = \frac{1}{2}m_a u_{||}^2 + \mu B + e_a\phi(\psi_*)$, where ψ has been safely replaced by $\psi_* = -J_3/e_a$ in the electric potential. The shift in the third angular pulsation has to be $\frac{\partial H}{\partial J_3} = -\frac{d\phi}{d\psi_*}$. As a final remark, it must be stressed that the radial electric field in a tokamak can be stronger, for instance in the plasma edge and/or in presence of a transport barrier. When the electric drift pulsation is upscaled, i.e. $v_E/a \sim \rho_*\Omega_c$, the bounce motion is affected, and the radial motion as well. The key parameter is in fact the shear of the radial electric field. It has mainly two consequences: a change of the condition of bouncing, and a squeeze of the trajectory radial extent of trapped particles, hence the name "orbit squeezing" given to this behaviour. More details can be found in [13, 14, 15]. It is interesting to consider the case of a "rigid" toroidal rotation of the plasma at speed $\mathbf{V} = -\frac{d\phi}{d\psi}R^2\nabla\zeta$. The corresponding toroidal angular frequency is a flux function $\Omega = -\frac{d\phi}{d\psi}$. Let us call $\mathbf{u}$ the velocity in the rotating frame of reference - the particle velocity $\mathbf{v}$ in the laboratory frame of reference is

$$\mathbf{v} = \Omega R^2\nabla\zeta + \mathbf{w}$$

The toroidal canonical momentum then reads

$$P_\zeta = -e_a\psi_* = -e_a\psi + m_a\frac{I}{B}w_{||} + m_a\Omega R^2$$

The Hamiltonian can then be recast as [16]

$$H = \frac{1}{2}m_a w_{||}^2 + \mu B + e_a\phi(\psi_*) - \frac{1}{2}m_a\Omega^2R^2$$

It thus appears that the modification of the precessional frequency is the same as the one found at low values of the rotation. However, an effective potential appears, the

last term in Eq.(19), which is not a flux function. It is responsible for changes in the bounce condition and radial shape of the trajectories. The energy shift $-\frac{1}{2}m_a R^2\Omega^2$ is the expected expression for the energy associated with the centrifugal force[26].

B Explicit expressions in a geometry of circular concentric magnetic surfaces

It is usually difficult to provide explicit expressions of the angular pulsations $\mathbf{\Omega}$, and even more to compute the angular variables. However a geometry of circular concentric magnetic surfaces at large aspect ratio offers this opportunity, and as such is quite often used to provide analytical results. It also shows the analogy with the pendulum. The magnetic field can be expressed in cylindrical coordinates as $\mathbf{B} = B_0 R_0/R\,(\mathbf{e}_\zeta + \epsilon(r)/q(r)\mathbf{e}_\theta)$, where $\epsilon = r/R_0 \ll 1$ is the inverse aspect ratio, and $\mathbf{e}_\zeta, \mathbf{e}_\theta$ are unit vectors in the toroidal and the poloidal direction. In the limit of large aspect ration, the norm of the field reduces to $B = B_0(1 - \epsilon\cos\theta) + o(\epsilon^2)$. Strictly speaking, θ is not a straight field line coordinate, but the geometric angle. These two angles differ by $o(\epsilon)$, so that they are considered the same in the following.

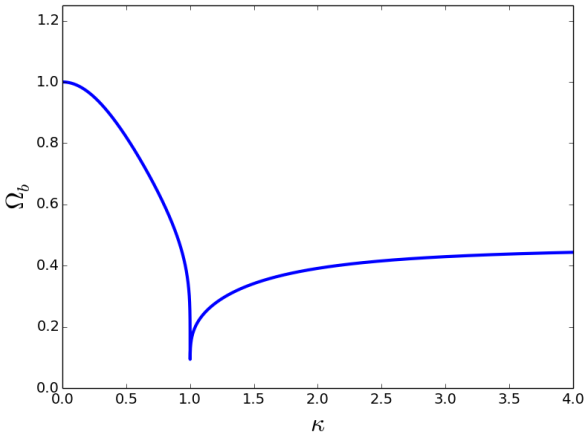

Figure 16: Transit/bounce pulsation vs trapping parameter κ.

B.1 Second angular pulsation and link between the poloidal and second angles

The magnetic drift is ignored so that the particle move along a field line on a magnetic surface $r = r_\star$, so that $\epsilon = r_\star/R_0$, and $q = q(r_\star)$. At lowest order in ϵ, the Jacobian is just $\mathcal{J} = 1/q(r)R_0$ so that the energy reads

$$E = \frac{1}{2}m_a q^2 R_0^2 \left(\frac{d\theta}{dt}\right)^2 + \mu B_0 b\,(\theta)$$

where $b\,(\theta) = 1 - \epsilon\cos\theta$. Trapping occurs when $\lambda_c \leq \lambda \leq \lambda_{\max}$, while particles are passing if $0 \leq \lambda \leq \lambda_c$, where $\lambda_c = \frac{1}{1+\epsilon}, \lambda_{\max} = \frac{1}{1-\epsilon}$. It is useful to introduce an alternative variable κ defined as

$$\kappa^2 = \frac{2\epsilon\lambda}{1 - \lambda(1-\epsilon)}$$

[26]Note that the sign minus comes from the correction associated with the angular frequency in the kinetic toroidal momentum

or equivalently

$$\lambda = \frac{\kappa^2}{2\epsilon + (1-\epsilon)\,\kappa^2}$$

Particles are passing if $0 \leq \kappa \leq 1$ and trapped if $1 \leq \kappa \leq +\infty$. The correspondence between λ and κ yields

$$1 - \lambda b(\theta) = \frac{2\epsilon}{2\epsilon + (1-\epsilon)\,\kappa^2}\left[1 - \kappa^2 \sin^2\left(\frac{\theta}{2}\right)\right]^{1/2}$$

so that the parallel velocity takes a convenient form

$$u_\parallel = \epsilon_\parallel v \left[\frac{2\epsilon}{2\epsilon + (1-\epsilon)\,\kappa^2}\right]^{1/2}\left[1 - \kappa^2 \sin^2\left(\frac{\theta}{2}\right)\right]^{1/2}$$

where $v = \sqrt{2E/m_a}$. For passing particles, the integrals run over the interval $[0, \pi]$, using up-down symmetry. It is then convenient to introduce the change of variable $u = \theta/2$, which spans $[0, \pi/2]$. This is not the best procedure for trapped particles, since in this case the integrals run over $[0, \theta_b]$, where $\sin(\theta_b/2) = 1/\kappa$. It is then better to use the change of variable $\sin v = \kappa \sin\left(\frac{\theta}{2}\right)$, where the new variable v spans $[0, \pi/2]$. The bounce/transit frequency can then be expressed in terms of the complete elliptical function of the first kind $\mathbb{K}$, namely $\Omega_b = \frac{v}{q(r_\star)R_0}\epsilon_\parallel \overline{\Omega}_b$ (the sign of the parallel velocity only matters for passing particles), where

$$\frac{1}{\overline{\Omega}_b}\left[\frac{2\epsilon + (1-\epsilon)\,\kappa^2}{2\epsilon}\right]^{1/2}\tau(\kappa)$$

with

$$\tau(\kappa) = \frac{2}{\pi}\left\{\begin{array}{cc} \mathbb{K}(\kappa^2) & 0 \leq \kappa \leq 1 \\ \frac{2}{\kappa}\mathbb{K}\left(\frac{1}{\kappa^2}\right) & 1 \leq \kappa \leq +\infty \end{array}\right.$$

and

$$\mathbb{K}(m) = \int_0^{\frac{\pi}{2}} \frac{du}{\sqrt{1 - m\sin^2 u}}$$

The reader should be warned that the "bounce" pulsation often given in the literature corresponds in fact to half a period, i.e. $\tau(\kappa) = \frac{2}{\pi}\frac{1}{\kappa}\mathbb{K}\left(\frac{1}{\kappa^2}\right)$. As expected, the bounce/transit period becomes very large near the passing/trapped boundary $\kappa = 1$ since $\mathbb{K}(\kappa) \simeq -\frac{1}{2}\ln|1-\kappa|$ for $|1-\kappa| \ll 1$. Let us recall also the limit values of elliptic values $\mathbb{E}(0) = \mathbb{K}(0) = \pi/2$ and $\mathbb{E}(1) = 1$. An example of dependence of $\overline{\Omega}_b$ with κ is shown on Fig.16. A useful expression of $\alpha_b(\theta)$ in the upper quadrant $0 \leq \theta \leq \frac{\pi}{2}$, $0 \leq \alpha_b \leq \frac{\pi}{2}$ is

$$\alpha_b = \left\{\begin{array}{cc} \pi\frac{\mathbb{F}\left(\frac{\theta}{2},\kappa^2\right)}{\mathbb{F}\left(\frac{\pi}{2},\kappa^2\right)} & \text{if } 0 \leq \kappa < 1 \text{ (passing)} \\ \frac{\pi}{2}\frac{\mathbb{F}\left(\sin^{-1}\left[\kappa\sin\left(\frac{\theta}{2}\right)\right],\frac{1}{\kappa^2}\right)}{\mathbb{F}\left(\frac{\pi}{2},\frac{1}{\kappa^2}\right)} & \text{if } 1 < \kappa < +\infty \text{ (trapped)} \end{array}\right.$$

where $F(\zeta, k)$ is the incomplete elliptical function of the first kind defined as

$$\mathbb{F}(\zeta, m) = \int_0^{\zeta} \frac{d\delta}{\sqrt{1 - m\sin^2\delta}}$$

This relation can be formally inverted to provide a link between the guiding-centre poloidal angle θ and the angular variable α_b. It is also interesting to construct this link for all values of the angles α_b and θ. Noting that $\mathbb{K}(m) = \mathbb{F}\left(\frac{\pi}{2}, m\right)$, the relation Eq.(19) can be rephrased as

$$\sin\left(\frac{\theta}{2}\right) = \left\{\begin{array}{cc} \mathrm{sn}\left(\frac{1}{2}\tau(\kappa)\alpha_b, \kappa^2\right) & 0 \leq \kappa < 1 \\ \frac{1}{\kappa}\mathrm{sn}\left(\frac{1}{2}\kappa\tau(\kappa)\alpha_b, \frac{1}{\kappa^2}\right) & 1 < \kappa < +\infty \end{array}\right.$$

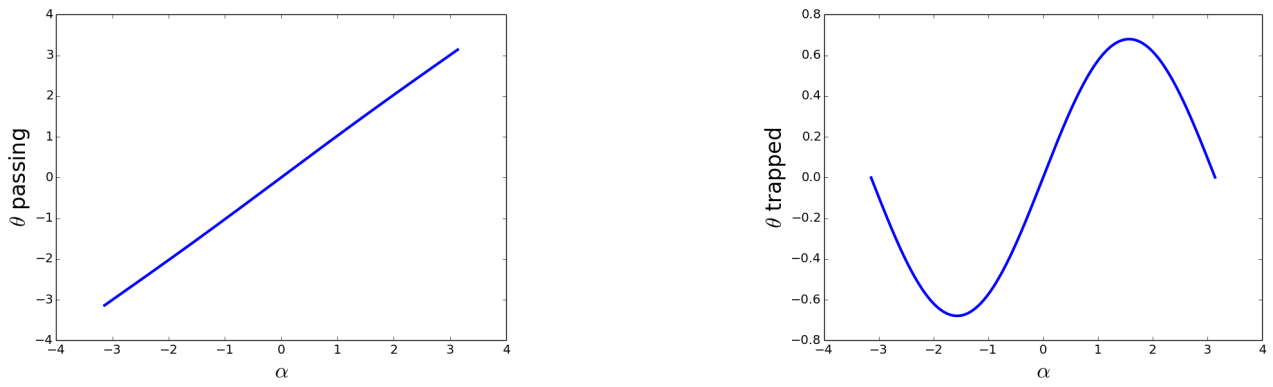

Figure 17: Left panel : Poloidal angle θ vs 3rd angle α_3 for a nearly freely passing particle $\kappa = 1/3$. Right panel : Poloidal angle θ vs 3rd angle α_3 for a deeply trapped particle $\kappa = 3$.

Notations	$\lambda = \frac{\mu B_0}{E}$	$\epsilon_c(\lambda)$	$\theta_b(\lambda)$	κ
Passing	$0 \leq \lambda \leq \lambda_c = \frac{1}{1+\epsilon}$	1	none	$0 \leq \kappa < 1$
Trapped	$\lambda_c \leq \lambda \leq \lambda_{\max} = \frac{1}{1-\epsilon}$	0	$-\pi < \theta_b < \pi$	$1 < \kappa < +\infty$

Table 2: Notations and conventions for passing and trapped particles.

valid for all α_b, θ. The function $\mathrm{sn}(\delta, m)$ is the Jacobian elliptic function that coincides with the trigonometric $\sin\delta$ function for $m \ll 1$, more precisely

$$\mathrm{sn}(\delta, m) = \sin\left[\left(1 - \frac{m}{4}\right)\delta + \frac{m}{8}\sin 2\delta\right] + o(m^2)$$

One recovers that $\theta = \alpha_b + \frac{1}{4}\kappa^2 \sin(\alpha_b)$ for deeply passing particles $\kappa \to 0$. For deeply trapped particles $\kappa \to \infty$, $\theta = \theta_b \sin\alpha_b$ where θ_b is the bounce angle, $\sin(\theta_b/2) = 1/\kappa$ (see Fig.17). Note that the Jacobi sn function differs significantly from a sinusoidal function for barely trapped or passing particles $\kappa \sim 1$ (see Fig.18). The derivative $\frac{d\alpha_b}{d\theta}$ reads

$$\tau(\kappa)\, d\alpha_b = \epsilon_{\|} \frac{d\theta}{\sqrt{1 - \kappa^2 \sin^2\frac{\theta}{2}}}$$

with $\epsilon_{\|}$ should be set to 1 for passing particles since it is already accounted for in the sign of Ω_b.

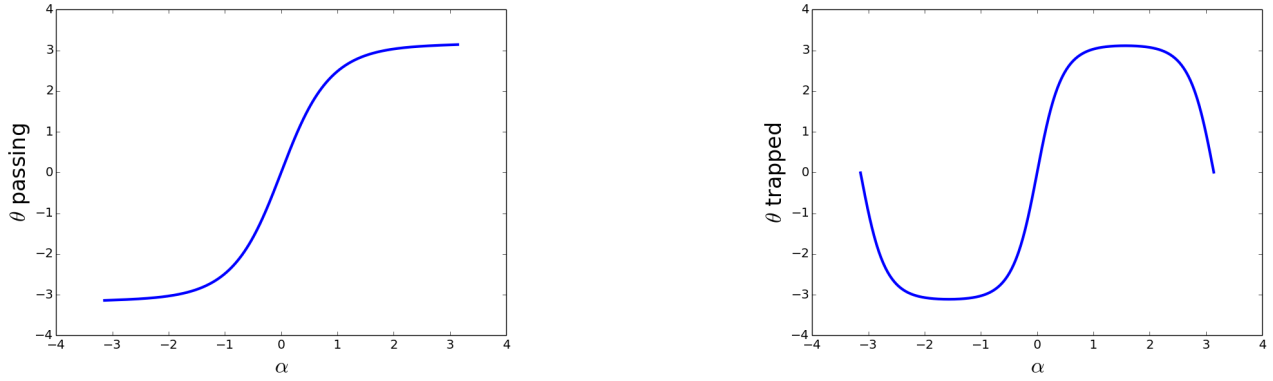

Figure 18: Left panel : Poloidal angle θ vs 3rd angle α_3 for a barely passing particle $\kappa = 0.9999$. Right panel : Poloidal angle θ vs 3rd angle α_3 for a barely trapped particle $\kappa = 1.0001$.

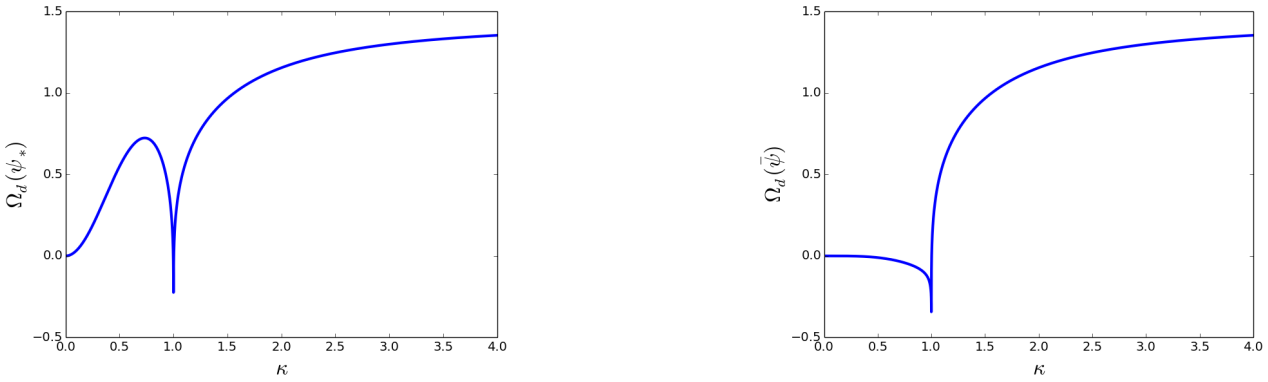

Figure 19: Magnetic drift pulsation versus trapping parameter κ. Left panel : the 3rd invariant of motion is ψ_*. Right panel : the 3rd invariant of motion is $\bar{\psi}$. Parameters are $\epsilon = 0.3$ and $s = 0.5$.

B.2 Third angular pulsation

The average magnetic drift pulsation Ω_d is defined as the time average of the pulsation Ω_α , which in a pressure-less large aspect ratio circular geometry of concentric magnetic surfaces reduces to

$$\begin{aligned}\Omega_\alpha(\mathbf{J},\theta) &= \frac{dq}{d\psi}\Omega_\theta\hat{\psi} + \mathbf{v}_D\cdot\nabla\zeta - q\mathbf{v}_D\cdot\nabla\theta \\ &= \frac{q}{r_\star}\frac{E}{e_a B_0 R_0}\left(2-\lambda b(\theta)\right)\cos\theta + \left.\frac{dq}{dr}\right|_{r=r_\star}\hat{r}\frac{d\theta}{dt}\end{aligned}$$

where $\hat{r} = \frac{q}{r_\star}\frac{m_a u_\parallel}{e_a B_0}R$. The pulsation Ω_α is of the form $\Omega_\alpha = \frac{q}{r_\star}\frac{E}{e_a B_0 R_0}\overline{\Omega}_\alpha$, where

$$\begin{aligned}\overline{\Omega}_\alpha(r_\star,\lambda,\theta) &= (2-\lambda b)\cos\theta + 2\frac{s}{\epsilon}(1-\lambda b)(1-\epsilon\cos\theta) \\ &= \lambda b\cos\theta + 2\frac{s}{\epsilon}(1-\lambda b) + 2(1-\lambda b)\cos\theta(1-s)\end{aligned}$$

Here $s = \left.\frac{rdq}{qdr}\right|_{r=r_\star}$ is the magnetic shear. The last term of the r.h.s. is a regular function in λ (no divergence near the trapped/passing boundary) and of order ϵ. It can therefore be ignored. Hence $\Omega_\varphi = \frac{q}{r_\star}\frac{E}{e_a B_0 R_0}\overline{\Omega}_d(\kappa)$, where

$$\begin{aligned}\overline{\Omega}_d(\kappa) &= \frac{1}{\int_0^{\frac{\theta_b}{2}}\frac{du}{\sqrt{1-\kappa^2\sin^2 u}}} \\ &\quad \int_0^{\frac{\theta_b}{2}}\frac{du}{\sqrt{1-\kappa^2\sin^2 u}}\frac{\kappa^2\left(1-2\sin^2 u\right)+4s\left(1-\kappa^2\sin^2 u\right)}{2\epsilon+(1-\epsilon)\kappa^2} \\ &= \frac{\kappa^2}{2\epsilon+(1-\epsilon)\kappa^2}\left\{\left(1-\frac{2}{\kappa^2}\right)+\frac{2}{\kappa^2}(1+2s)\frac{\int_0^{\frac{\theta_b}{2}}du\sqrt{1-\kappa^2\sin^2 u}}{\int_0^{\frac{\theta_b}{2}}\frac{du}{\sqrt{1-\kappa^2\sin^2 u}}}\right\}\end{aligned}$$

where $\theta_b = \pi$ for passing particles. The function $\overline{\Omega}_d(\kappa)$ can then be expressed as a combination of complete elliptic functions of second and first species.

For passing particles $0 \le \kappa \le 1$ one gets

$$\overline{\Omega}_d(\kappa) = \frac{\kappa^2}{2\epsilon+(1-\epsilon)\kappa^2}\left\{1+\frac{2}{\kappa^2}\left(\frac{\mathbb{E}(\kappa^2)}{\mathbb{K}(\kappa^2)}-1\right)+4s\frac{\mathbb{E}(\kappa^2)}{\mathbb{K}(\kappa^2)}\right\}$$

For trapped particles $1 \le \kappa \le \infty$, the result is

$$\overline{\Omega}_d(\kappa) = \frac{\kappa^2}{2\epsilon+(1-\epsilon)\kappa^2}\left\{2\frac{\mathbb{E}\left(\frac{1}{\kappa^2}\right)}{\mathbb{K}\left(\frac{1}{\kappa^2}\right)}-1+4s\left[\frac{1}{\kappa^2}-1+\frac{\mathbb{E}\left(\frac{1}{\kappa^2}\right)}{\mathbb{K}\left(\frac{1}{\kappa^2}\right)}\right]\right\}$$

These results apply for the choice $J_3 = -e_a\psi_*$. As mentioned in the Appendix A, a wiser choice is to choose a reference magnetic surface as the time average of the guiding-center radial position. In this case, one has $\hat{r} = \frac{q}{\bar{r}}\left[\frac{m_a u_\parallel}{e_a B_0}R - \left\langle \frac{m_a u_\parallel}{e_a B_0}R \right\rangle\right]$. This choice does not change the precession frequency of trapped particles since the time average of the parallel velocity vanishes. However it does modify the magnetic drift pulsation of passing particles, which becomes

$$\begin{aligned}\overline{\Omega}_d(\kappa) &= \frac{\kappa^2}{2\epsilon + (1-\epsilon)\,\kappa^2}\left\{1 + \frac{2}{\kappa^2}\left(\frac{\mathbb{E}(\kappa^2)}{\mathbb{K}(\kappa^2)} - 1\right)\right. \\ &+ \left. 4s\left[\frac{\mathbb{E}(\kappa^2)}{\mathbb{K}(\kappa^2)} - \left(\frac{\pi}{2\mathbb{K}(\kappa^2)}\right)^2\right]\right\}\end{aligned}$$

The difference of convention in the choice of reference magnetic surface explains the different expressions of magnetic drift curvature pulsation found in the literature. The magnetic drift pulsation associated with ψ_* agrees with [17], while the version with $\bar{\psi}$ agrees with [18]. The latter is close to [19], up to the term $\left(\frac{\pi}{2\mathbb{K}(\kappa^2)}\right)^2$ replaced by $\frac{\pi}{2\mathbb{K}(\kappa^2)}\sqrt{1-\kappa^2}$. Corrections due to the Shafranov shift can be found in [19]. An example is shown on Fig.(19).

References

[1] L.D. Landau and E.M. Lifshitz. *The Classical Theory of Fields*. Pergamon Press, 1971.

[2] H. Goldstein. *Classical Mechanics*. Addison-Wesley, 1980.

[3] V.I. Arnold. *Mathematical Methods of Classical Mechanics*. Springer, 1978.

[4] R. G. Littlejohn. Hamiltonian formulation of guiding center motion. *The Physics of Fluids*, 24(9):1730–1749, 1981.

[5] M. Kruskal. Asymptotic theory of hamiltonian and other systems with all solutions nearly periodic. *Journal of Mathematical Physics*, 3(4):806–828, 1962.

[6] A. J. Lichtenberg and M. A. Lieberman. *Regular and Stochastic Motion*. Springer, 1983.

[7] R. G. Littlejohn. Variational principles of guiding centre motion. *Journal of Plasma Physics*, 29(1):111–125, 1983.

[8] T. G. Northrop and J. A. Rome. Extensions of guiding center motion to higher order. *The Physics of Fluids*, 21(3):384–389, 1978.

[9] R.J Goldston and P.H Rutherford. *Introduction to Plasma Physics*. CRC Press, 1995.

[10] R.D. Hazeltine and J.D. Meiss. *Plasma Confinement*. Dover, 1992.

[11] R.B. White and L. E. Zakharov. Hamiltonian guiding center equations in toroidal magnetic configurations. *Physics of Plasmas*, 10(3):573–576, 2003.

[12] M. V. Berry. Regular and irregular motion. *AIP Conference Proceedings*, 46(1):16–120, 1978.

[13] H. L. Berk and A. A. Galeev. Velocity space instabilities in a toroidal geometry. *The Physics of Fluids*, 10(2):441–450, 1967.

[14] K. C. Shaing and R. D. Hazeltine. Effects of orbit squeezing on ion transport in the banana regime in tokamaks. *Physics of Fluids B: Plasma Physics*, 4(8):2547–2551, 1992.

[15] M. Landreman and P. J. Catto. Trajectories, orbit squeezing and residual zonal flow in a tokamak pedestal. *Plasma Physics and Controlled Fusion*, 52(8):085003, jun 2010.

[16] S. Lanthaler, J. P. Graves, D. Pfefferlé, and W. A. Cooper. Guiding-centre theory for kinetic-magnetohydrodynamic modes in strongly flowing plasmas. *Plasma Physics and Controlled Fusion*, 61(7):074006, may 2019.

[17] C. Nguyen. *Magneto-hydrodynamic activity and energetic particles : application to Beta Alfven Eigenmodes*. Ecole Polytechnique, 2009.

[18] A. Merle. *Stability and properties of electron-driven fi shbones in tokamaks*. Ecole Polytechnique, 2012.

[19] F. Zonca, P. Buratti, A. Cardinali, L. Chen, J.-Q. Dong, Y.-X. Long, A.V. Milovanov, F. Romanelli, P. Smeulders, L. Wang, Z.-T. Wang, C. Castaldo, R. Cesario, E. Giovannozzi, M. Marinucci, and V. Pericoli Ridolfini. Electron fishbones: theory and experimental evidence. *Nuclear Fusion*, 47(11):1588–1597, oct 2007.